TANDEM
ACCELERATOR LABORATORY
ANNUAL REPORT
1980

GREEK ATOMIC
ENERGY COMMISSION

N.R.C "DEMOKRITOS"

NUCLEAR RESEARCH CENTER DEMOKRITOS

TANDEM ACCELERATOR LABORATORY

ANNUAL REPORT 1980

Editor: G.S. Anagnostatos

I N D E X

INTRODUCTION

The areas of research, established in our laboratory a few years back, were followed also during 1980. Appreciable emphasis however was given in the area of applications of nuclear methods.

This emphasis is not the result of staff expansion as much as the desire of the researchers to utilize their knowledge in tackling problems of their immediate environment.

In this area, XRF, PIXE, perturbed angular correlations as well as nuclear reactions were utilized leading to significant conclusions in many instances.

In the areas of basic research, work continued along the lines established in the previous years. In heavy ions, measurements were extended in other nuclei in the search of quasi-molecular resonances -a topic of an International Conference organized by the Laboratory in June 1980. Similarly the competition between pn and d channels was studied in other systems. The results of these experiments indicate that measurement of the competition offers the possibility of distinction between compound nucleus and direct reaction mechanisms. Spectroscopic work with gamma rays emitted either from light or heavy ion reactions resulted in establishing decay schemes for several nuclei. In theory research has been performed in correlating magic numbers with symmetries in the isomorphic model, the establishment of a two-nucleon effective potential for high energy heavy - ion collisions and further extensions of the isomorphic and VMI models.

From a technical point of view, we had very few mishaps serious enough to hamper our operation. We feel however strongly the energy limitations imposed on us by the low terminal voltage and we still hope that adequate funds can be secured in the near future for the necessary post accelerator.

Concerning our data acquisition system, the on-line PDP-15 computer is clearly showing signs of its age and an order has been placed for the procurement of a new more powerful computing system.

Visits of scientists from abroad for experiments with our Tandem as well as visits by our scientists to other laboratories, were found again to be very beneficial.

The dedication and quality of our technical and administrative personnel, this hidden variable in the continuous progress of our laboratory, is especially acknowledged.

George Vourvopoulos

I. HEAVY ION REACTIONS

Search for intermediate structure in ^{36}Ar above the coulomb barrier

G. Vourvopoulos, X. Aslanoglou , R. Caplar[+] and D. Pocanic[+]

The reaction $^{24}Mg(^{12}C,\alpha)\ ^{32}S$ leading to the ground and first excited states of ^{36}Ar was utilized. The excitation function covered the region E_{CM}= 11.9 - 19.4 MeV and angular distributions were measured at 16 angles ($\theta_L = 10^o - 85^o$).

The measured excitation functions were analyzed statistically. For this purpose, the summed absolute correlation function C(E), the summed correlation function C'(E), the summed absolute deviation function D(E) and the summed deviation function D'(E) were calculated. The results are shown in Figure 1.

The measured angular distributions were fitted with squares of single Legendre polynomials and with squares of the coherent sums of pairs of Legendre polynomials ($\sigma(\theta) = k.|\ P_\ell(\cos\theta) + \alpha e^{i\beta} P_{\ell'}(\cos\theta)|^2$) For each angular distribution, ℓ and ℓ' ($\ell' = \ell + 1$ or $\ell' = \ell + 2$) as well as α and β were varied in order to find the best fit to the data. The results are shown in Figure 2.

The present experiment and the subsequent analysis show the following: (i) in most cases, two-level fits to the angular distributions are satisfactory, (ii) single ℓ-values, i.e. ℓ = 5,4,7,9,11 and 13 are predominant ($\alpha < 0.5$, or $\alpha > 2$) in the angular distribution at E_{CM}= 12.3, 12.9, 14.3, 16.4, 18.1 and 18.7 MeV respectively; (iii) maxima in the deviation functions appear at the same energies as above, none of them however exceeds the 1% probability limit. Thus, the data and the analysis indicate the presence of spin selectivity in the reaction and energy range studied. However, intermediate resonances in the ^{36}Ar composite system, if present, seem to be relatively weak and probably interfere with the statistical background.

[+]R. Boskovic Institute, Zagreb, Yugoslavia

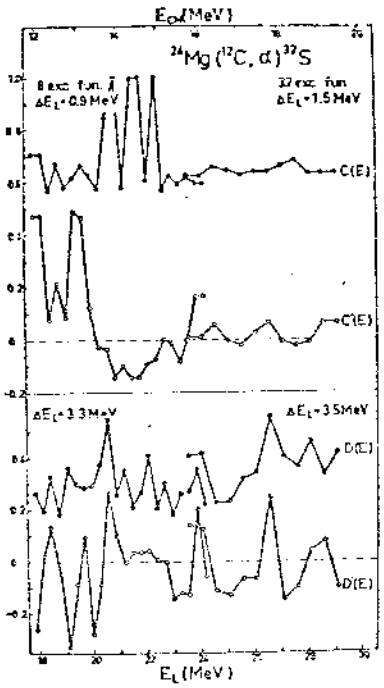

Fig. 1

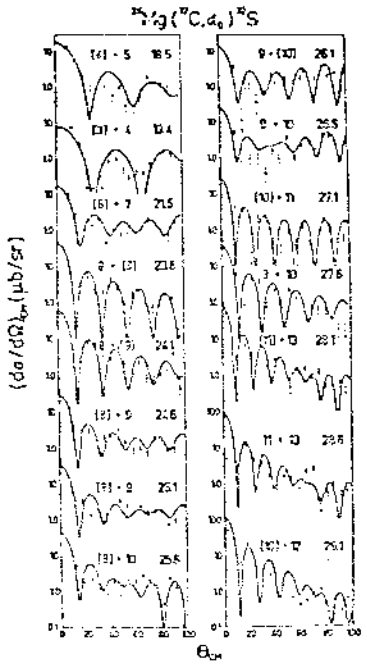

Fig. 2

Fig. 1. Results of statistical analysis.

Fig. 2. Fits with coherent sums of pairs of Legendre polynomials at indicated laboratory energies; the values without parentheses denote the Legendre polynomials having larger amplitudes.

The contribution of unbound deuteron disintegration to the reaction $^{12}C(^{16}O,pn)\ ^{26}Al$.

E.N. Gazis, P. Kakanis and A.C. Xenoulis

A proton-neutron pair can be emitted in a nuclear reaction via two distincly different processes: either via succesive evaporation of nucleons or from the disintegration of singlet deuterons as soon as the latter are found outside the potential of the residual nucleus.

In a previous experimental study[1] of the reaction $^{12}C(^{16}O,pn)$ at 30 and 36 MeV it was concluded that a significant fraction of its cross section was due to the emission and subsequent decay of unbound deuterons. According to evaporation model estimates, however, only a small fraction, between 3 and 10% relative to the stable deuteron emission is expected to proceed via singlet deuteron emission.

In the present study proton-neutron coincidence techniques were utilized in order to observe the fraction of pn originating from singlet deuteron disintegration. The different angular dependence of a proton and a neutron emitted either succesively or via disintegration of a singlet deuteron was exploited in order to characterize the process by which the proton-neutron pairs were produced. Although pn-coincidence data were obtained at several angles , special attention was given to symmetric detection geometries, that is $\theta_p = \theta_n$ and $\theta_p = -\theta_n$ about the beam axis.

From the pn-coincidence angular distribution and the energy distribution of protons it was concluded that the proton-neutron pairs emitted in the reaction are almost exclusively due to succesive evaporation of nucleons from the compound nucleus.

Reference

1. V.Valcovic, R.L. Liebert, R.Plasek, R.M. Wheeler, T. Zaber and G.C. Phillips, Lett. Nuov. Cim 10, 461 (1974).

The systematics of the competition between pn and d isoproduct emission in heavy-ion induced compound-nucleus reactions

A.C. Xenoulis and A. Aravantinos

The particle-γ coincidence technique recently proposed[1] for the measurement of isoproduct competition, i.e. the competition between exit channels producing the same residual nucleus, has been employed in order to obtain the competition between pn and d emission in a series of heavy ion induced CN reactions.

These data demonstrate that, in general, the pn relative to d emission increases with increasing bombarding energy. Furthermore, a representation , which seems to be unique, was recognized by which the pn over d competition data are unified irrespectively of the nuclear reaction involved. Specifically, when the logarithm of the ratio σ_{pn}/σ_d is associated with the maximum excitation energy available in the residual nucleus a nearly straight line dependence is observed. It should be noted that almost all the available data are restricted on a unique line irrespectively of the reaction.

There is mounting indication that the factor underlying the isoproduct competition is the phase space of density of states available to the cluster or multiparticle evaporation.

This recent understanding with respect to isoproduct competition in CN reactions offers firstly a predictive framework for practical applications and secondly renders the measurements of pn over d emission a novel tool for the investigation of phenomena deviating from CN evaporation, such as competing reaction mechanisms or quasi-molecular resonances.

Reference

1. A.C. Xenoulis, E.N. Gazis, P. Kakanis, D. Bucurescu and A. Panagiotou, Phys. Lett. 90B, 224 (1980)

Distinction between compound-nucleus and direct reaction mechanisms in (^{6}Li,pn/d) reactions

A. Aravantinos and A.C. Xenoulis

The measurement of competition between pn and d emission in a heavy-ion induced reaction offers a possibility to distinguish between compound-nucleus and direct reaction mechanisms, in particular (^{6}Li,pn/d) reactions, since it is expected that the σ_{pn}/σ_{d} ratio will be very different in case of CN evaporation and direct ^{4}He transfer. In fact, we have developed a method for the measurement of competition between different reaction mechanisms in such reactions.

Of the reactions studied the ^{16}O(^{6}Li,pn/d) presents particular interest, which was studied as a function of bombarding energy between 10 and 19 MeV. In that reaction it has been observed that between 10 and 15 MeV it proceeds exclusively via compound-nucleus mechanism. At about 16 MeV the onset of competition between CN and direct mechanism is noticed, after which the direct mechanism progressively increases with increasing bombarding energy.

*Shape dependence of the ^{7}Li - ^{51}V reaction cross section**

E. Kossionides[+], K.H. Moebius, R. Boettger, P. Egelhof, Z. Moroz[++], D. Pressinger, E. Steffens, H. Gemmeke[‡], I. Koenig[‡], D. Fick[‡]

It has been shown[1] that the total reaction cross-section betwen an aligned ^{7}Li beam and ^{51}V depends on the orientation of the deformed incoming ^{7}Li nuclei. In order to investigate the dependence in greater detail, the angular distributions of light charged particles produced by the reaction were measured at E_{lab}= 12 and 20 MeV.

Preliminary evaluations of the analysing power $T_{20}(\theta)$ show that it is assymetric around 90° for all types of detected particles (p,d,t,α). The trend from positive values at the forward angles to negative values at the back can be interpreted within a semiclassical shape model (also used for the interpretation of the elastic scattering[2]) and the assumption of a direct reaction mechanism. It seems, therefore, that the analyzing power is dominated by the direct components of the reaction.

The detailed analysis of the results is still in progress.

References

1. K.-H. Moebius et al. "Shape effects in the ^{7}Li - ^{51}V reaction cross section". Contribution to the Fifth International Symposium on Polarization Phenomena in Nuclear Physics, Santa Fé, New Mexico, USA, 1980.
2. K.-H. Moebius et al. Phys. Rev. Let. 46 (1981) 1064

* Work performed at the Max-Planck -Institut fuer Kernphysik, D-6900 Heidelberg
+ Alexander von Humbold fellow, on leave of absence from NRC"Demokritos"
++ On leave of absence from Inst. of Nucl. Research , Warsaw, Poland.
‡ Fachbereich Physik, Philipps, Universitaet, D-3550 Marburg

High spin states in ^{69}Ga.*

P.Bakoyeorgos, P. Assimakopoulos[+], and T. Paradellis

The $^{64}Ni+^{7}Li$ reaction at 18 MeV Li bombarding energy has been used to populate high spin states in ^{69}Ga via the 2n exit channel.

Gamma-gamma coincidence experiments have established the decay scheme of the nucleus. Angular distribution experiments along with an extensive experimental set of attenuation coefficients obtained by different reactions have been used to obtain information on spin and mixing ratios of transitions deexciting the above mentioned levels.

Doppler shift attenuation experiments have been performed and mean lives of some excited levels have been also deduced. In Fig. 1 the resulting decay scheme of ^{69}Ga is shown.

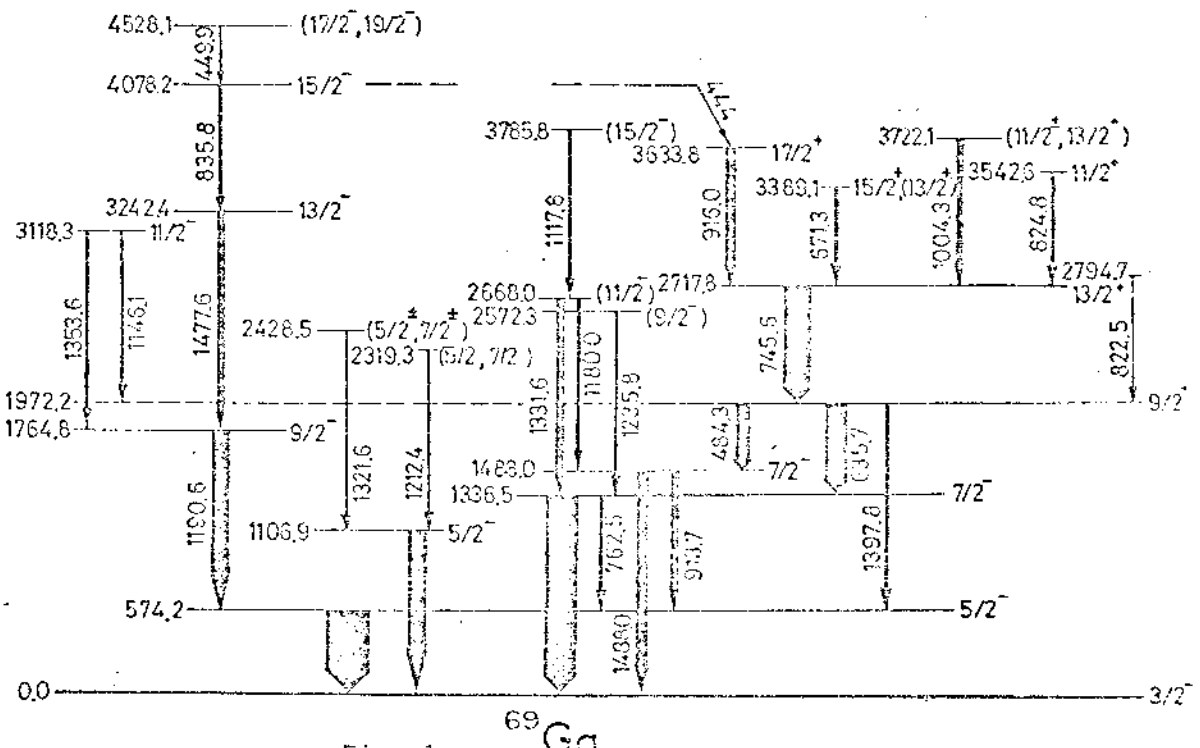

Fig. 1

* Part of a PH.D. thesis of one of the authors (P.B).

+ University of Ioannina

Mean lives of excited states populated in (p,γ) reactions on semithick targets

T. Paradellis

In (p,γ) reactions on semithick targets many states in the compound nucleus are excited which subsequently decay to the lower lying discrete states.

In the present work the reactions $^{56}Fe(p,\gamma)\ ^{57}Co$, $^{62}Ni(p,\gamma)\ ^{63}Cu$ $^{66}Zn(p,\gamma)\ ^{67}Ga$ and $^{68}Zn(p,\gamma)\ ^{69}Ga$ have been used to measure the attenuated Doppler shift of the γ rays which deexcite the lower lying states of these nuclei which have very well known measured mean lives. The data have been taken with targets of about $4mg/cm^2$ thickness and at a bombarding energy of 3 MeV.

In Fig.1 and 2 the experimental $F(\tau)$ versus τ data point are shown for several γ-rays from the four above mentioned reactions. Also the calculated theoretical $F(\tau)$ curves are drown for several assumptions of the delay time introduced by the cascading γ rays from the continuum (side feeding). From the overall picture it is concluded that an assumption of a side feeding of $\tau = 20 \pm 5$ fs reproduced nicely the experimental points for all reactions.

The results of this investigation shows that the (p,γ) reaction on semithick targets may provide important information on mean lives of states which cannot be otherwise populated by other reactions.

The method has been applied for the case of ^{69}Ga(see next article).

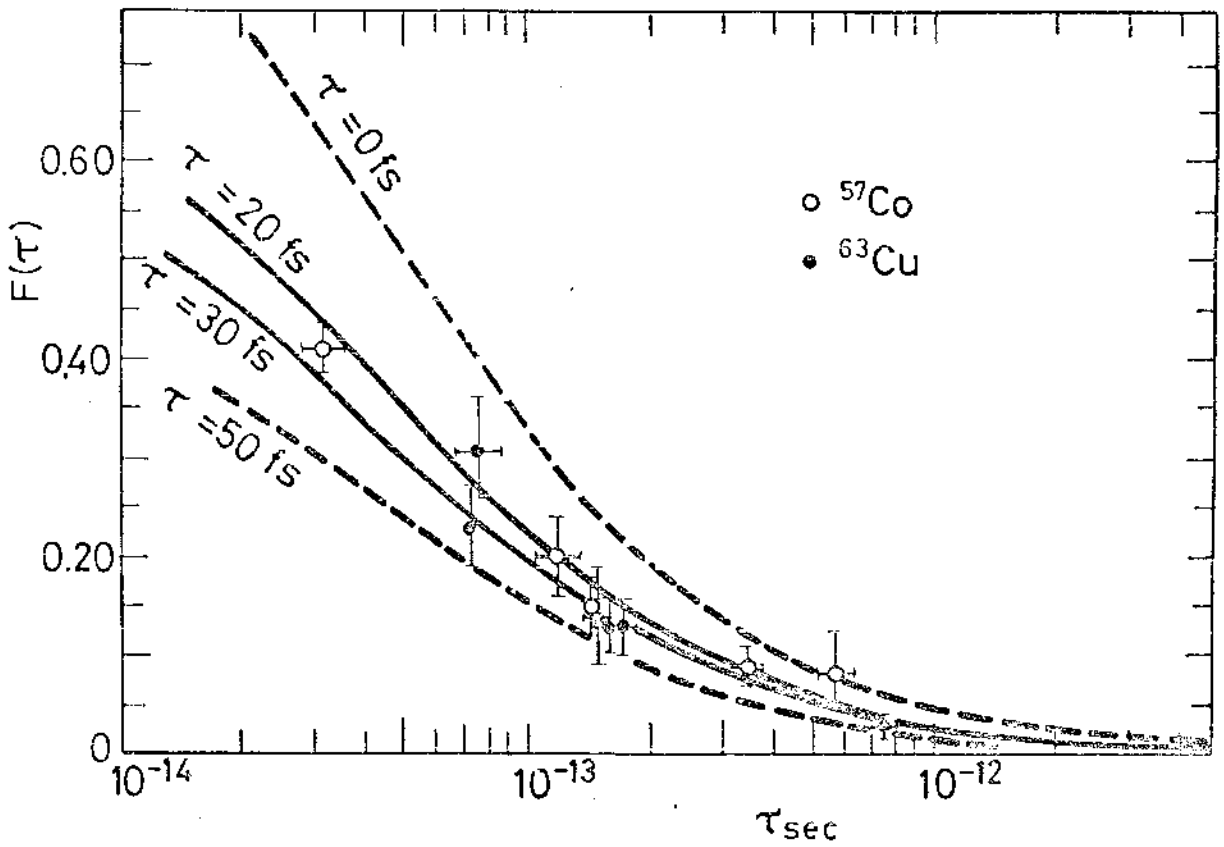

Fig. 1

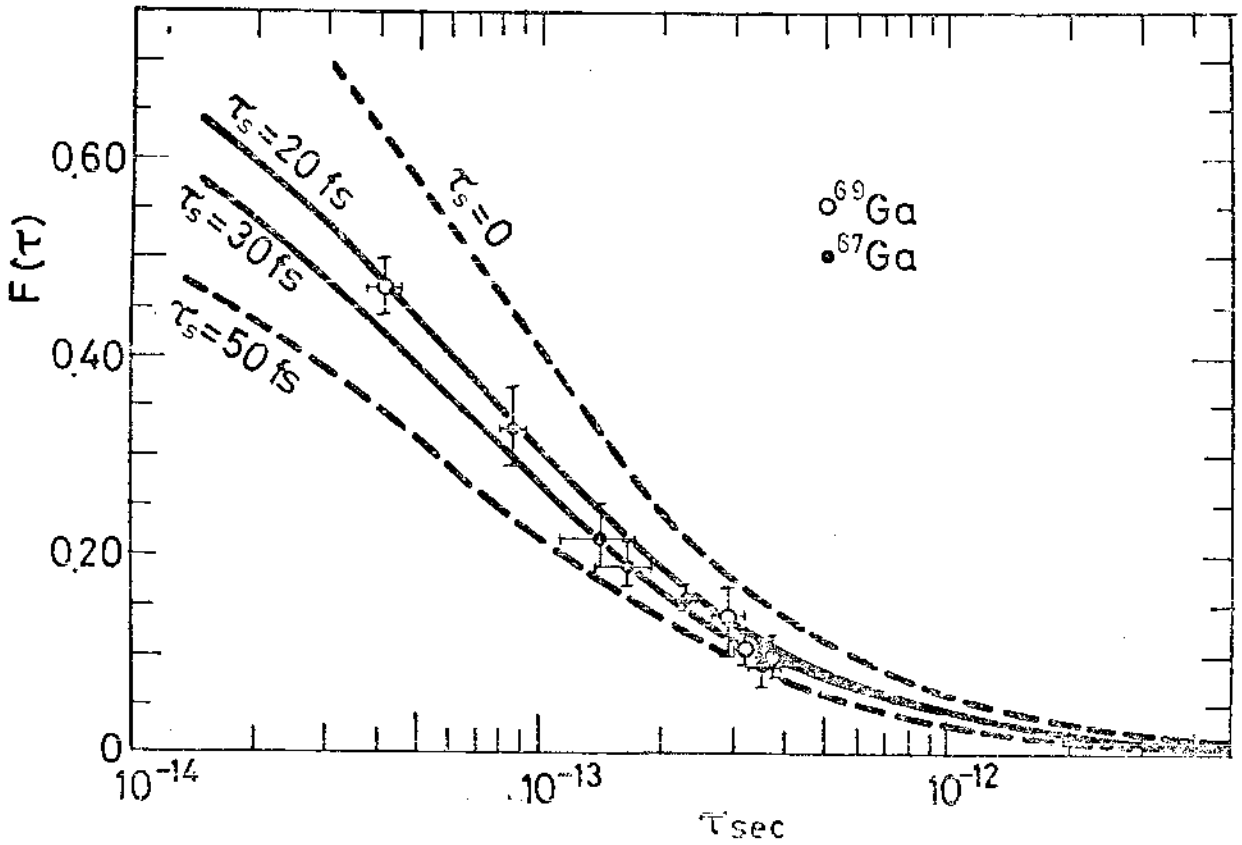

Fig. 2

Excited states in ^{69}Ga

T. Paradellis, G. Vourvopoulos

The $^{68}Zn(p,\gamma)$ ^{69}Ga reaction has been used to populate excited states in ^{69}Ga. Targets of $4mg/cm^2$ thickness have been used for angular distribution measurements. The analysis of the angular distribution data has been made on the basis of experimental alignment attenuation factors as derived in a previous work[1], Several spin and parities have been deduced for levels up to 2.6 MeV. For many transitions mixing ratios have been determined. In Fig.1 the resulting decay scheme is given.

From an analysis of the Doppler shift of γ-rays deexciting lower lying states in (p,γ) reactions it has been concluded that reliable mean lives of states can be obtained upon an assumption of a side feeding time of 20 fs from the continuum. (see Fig.2 previous paper)

In Table I, results for the excited states of ^{69}Ga are given. These results have been derived from the measured $F(\tau)$ values in the $^{68}Zn(p,\gamma)$ reaction with a side feeding time of $\tau = 20 + 5$ fs.

Reference

(1) T. Paradellis, G. Vourvopoulos, Fizika 10 Supp.(1978) 29

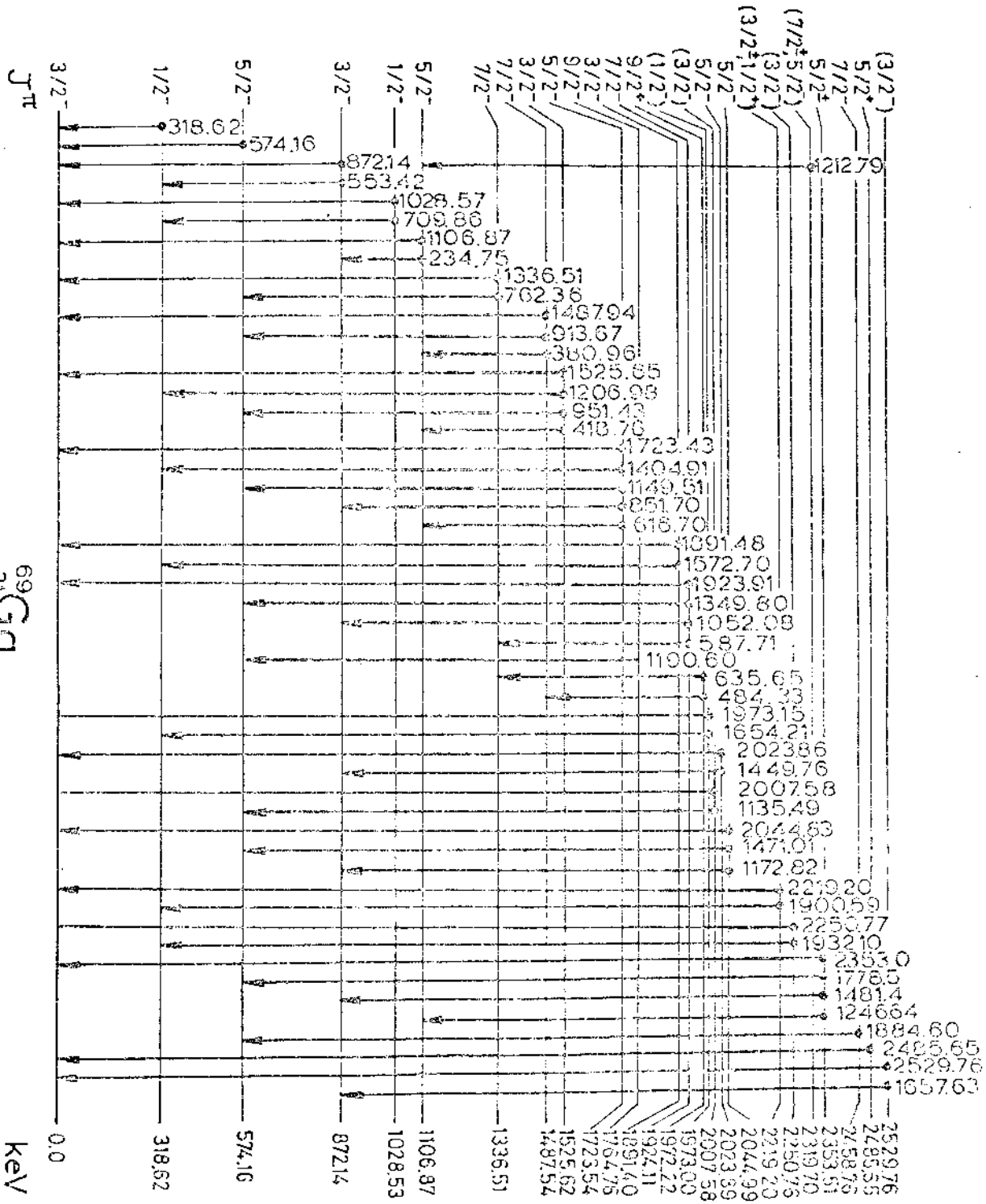

Fig. 1

Table I Mean lives of ^{69}Ga levels, obtained by DSAM from centroid shift measurements in singles spectra.

Level keV	J^{π}	γ-rays used keV	P(τ)	τ fs	τ Ref.Fluor. fs
1525.62	$3/2^-$	1525.6, 1207	0.03 (3)	≥400	≥3500
1723.54	$5/2^-$	1723.3,1405,1149	0.02 (1)	≥1400	1300(450)
1891.41	$3/2^-$	1891.5,1572.7	0.47 (3)	42 (8)	42 (4)
1924.11	$7/2^-$	1349.8,1052.0	≤ 0.05	≥900	≥350
1973.00	$(1/2)^-$	1973.0,1654.2	0.24 (4)	140 (40)	200(45) if J= 1/2, 400(90) if J=3/2
2007.6	$(3/2)^-$	2007.5,1135.5	0.08 (3)	510^{+300}_{-150}	490(70) if J= 3/2, 730(102)if J=5/2
2023.89	$5/2^-$	2023.9	0.14 (4)	280^{+120}_{-70}	290 (30)
2044.92	$5/2^-$	2044.9,1471.0,1172.8	0.22 (2)	160 (20)	193 (30)
2219.20	(3/2,1/2)	1900.6	0.07 (5)	≥300	
2250.76	$(3/2)^-$	2250.76,1932.1	0.24 (6)	140^{+70}_{-40}	
2319.70	$(5/2^-,7/2^{\pm})$	1212.8	≤ 0.12	≥300	
2353.51	$5/2^{\pm}$	1461.4,1246.6	≤ 0.15	≥250	
2458.76	$7/2^-$	1884.60	0.17 (9)	220^{+280}_{-80}	
2485.65	$5/2^+$	2485.65	0.30 (10)	100^{+80}_{-40}	
2529.76	$(3/2)^-$	2529.8,1657.6	0.29 (5)	110 (30)	

Structure and electromagnetic properties of ^{96}Ru

A.C. Xenoulis, E. Adamides, C.T. Papadopoulos[+] and R. Vlastou[+]

An experimental study of levels and electromagnetic properties of transitions in ^{96}Ru is in progress via spectrometry of prompt γ rays emitted in the reaction $^{96}Ru(p,p'\gamma)$.

Lifetimes of excited states were determined via the Doppler-shift attenuation method from energy shifts of γ rays as a function of angle of observation.

Analysis of angular distributions yielded mixing ratios and J^{π} values.

+ National Technical University of Athens

Relative dating of bones from Thessaly

Y. Maniatis[+] and A. Katsanos

Two human bones and one hyena bone fround in the same place at the banks of the river Pinios in Thessaly were relatively dated using their nitrogen-carbon-hydrogen and fluorine and uranium content (Table I). For the fluorine the Tandem Accelerator was used to bombard the sample with protons and thus to estimate the fluorine content from the characteristic gamma rays emitted from the reaction $^{19}F(p,\alpha\gamma)\ ^{16}O$ ( ). The uranium and other trace elements were determined by Proton Induced X-ray Emission (.

The chronological order determined for the bones agreed very nicely with the anthropological observation thus encouraging the use of these techniques for this kind of dating.

TABLE I

Carbon, hydrogen, nitrogen and fluorine contain of bones from Thesally.

Sample	C (%)	H (%)	N (%)	F (%)
New goat	15.99	2,47	4.47	-
Skull 2	9.94	1.34	2.73	0.44
Skull 1	6.69	0.88	1.29	0.45
Hyena	2.80	0.20	_	2.10

[+]Solid State Spectroscopy Lab., NRC Democritos

Technological examination of Ayia Irene terra cotta samples

Y. Maniatis[+] and A. Katsanos

Scanning Electron Microscopy and Infrared Spectroscopy were used for the examination of the Ayia Irene Terra Cotta samples in order to obtain information about the firing conditions applied in their manufacture. The combination of these two techniques has been proved very usefull in this case for technological studies. In addition Proton Induces X-ray Emission (PIXE) elemental analysis was applied for the composition of the samples.

The examination of fresh-factured surfaces of ceramic samples under the Scanning Electron Microscope (SEM) provides information on the internal morphology of the clays developed during firing and the degree of vitrification. This information combined with known morphologies of clays and pottery or by refiring pieces of samples in the laboratory and reexamination with the SEM lead to the determination of the firing temperatures used in Antiquity. In addition the degree of vitrification (or amount of glass) present in the microstructure of a fired clay body gives information about its strength, hardness and porosity which are associated with the use of the object and its state of preservation.

Furthermore the information obtained with the Proton Induced X-ray Emission analysis (PIXE) apart of helping to distinguish between groups of composition, provides data on the type of clay used, i.e. calcareous or non-calcareous and low or high refractory. These properties which affect the internal morphology developed during firing (Maniatis and Tite 1978) are needed for a more accurate estimate of the firing temperature without repeated refirings in the laboratory .

The Infrared spectra provide information on the presence or not of hydroxyl water in the clay mineral lattice (Grim 1968, Farmer 1979) and can therefore verify whether dehydroxylation or not has been accomplished. This if combined with the SEM results assists the assignment of low firing temperature ranges below the onset of vitrification.

With the combination therefore of the above techniques firing temperatures have been assigned as follows: (1) Sherds exhibiting initial vitrification: 750-800°C (2) sherds non-vitrified but completed dehydroxylation: 650-750°C and finally (3) Sherds non-vitrified and not completed dehydroxylation: below 650° C. Table 1 shows the concentrated results of the above techniques and the firing temperatures estimated. The samples have been grouped on archaeological grounds according to Mrs Caskeys classification. It is interesting to observe the consistancy of firing temperatures within each group. Although in general the firing temperatures are not very different to indicate different technologies from group to group the similarity of firing temperatures within each group emphasizes probably the slightly different prevailing firing conditions and seem to verify in a very good degree the archaeological classification. The slight differences also in Ni, Zn and Rb content between the main groups (Table 2) is indicative of a different clay source but certainly local could further tentatively indicate the production of these statues at different parts of the island and this would hence explain the slightly different firing conditions.

However, the above assumptions should be treated very cautiously because, firstly the compositional differences are not very reliable since the samples are very coarse and inhomogeneous and secondly the big size of these statues could present problems in keeping the firing temperature or atmosphere constant all around them.

In general this work has also proved the usefulness of the combination of the SEM and infrared techniques for the low fired ceramics.

+Solid State Spectroscopy Lab., NRC Demokritos

TABLE 1

Concetrated results on Ayia Irene terra cotta statues

Sample	Colour	Dehydroxylation	Vitrification	Firing Temp. (°C)
Group 1				
TC5	Dark Brown	Complete	IV	750-800
TC11	Grey	"	IV	750-800
TC14	Red-Grey	"	IV	750-800
TC18	" "	"	IV	750-800
TC19	Red	"	IV	750-800
Group 3-4-3/4				
TC4	Red Brown	Incomplete	NV	<650
TC7	" "	"	"	<650
TC12	" "	"	"	<650
TC17	" "	"	"	<650
TC15	Red	Complete	"	650-750
Group 5				
TC13	Red-Grey	Complete	IV	750-800
Group 6				
TC6	Grey	Complete	IV	750-800
Group 8				
TC1	Grey	Complete	NV	650-750
TC3	Dark Brown	"	"	650-750
TC8	Red-Grey	"	"	650-750
TC9	Dark Brown	"	"	650-750
TC10	Grey-Red	"	"	650-750
TC16	Dark Brown	"	"	650-750
Group 15				
TC1a	Brown	Complete	IV	750-800
TC2a	Red	"	"	750-800

TABLE 2

PIXE analysis of Ay.Irene terra cotta samples

SAMPLE	K	Ca	Ti	V	Mn	Fe	Ni	Zn	Rb	Sr	Zr
		(% weight)						(ppm)			
Group-1											
TC5	2.6	0.99	0.30	0.018	0.06	7.0	89	58	53	108	38
TC11	3.3	0.49	1.36	0.040	0.06	7.6	118	122	56	41	93
TC14	2.6	0.54	0.40	0.022	0.38	9.0	103	101	56	170	45
TC18	3.4	0.40	0.31	0.021	0.08	8.1	148	118	53	31	77
TC19	3.3	0.36	0.29	0.017	0.09	7.9	141	84	49	32	54
Group 3-4-3/5											
TC4	3.7	0.47	0.32	0.026	0.13	7.5	68	39	72	29	96
TC7	3.3	0.55	0.37	0.026	0.12	6.9	70	95	75	44	118
TC12	2.6	1.1	0.30	0.019	0.08	7.1	81	61	54	56	-
TC17	3.4	0.41	0.29	0.021	0.14	7.9	101	46	70	42	66
TC15	3.4	0.45	0.31	0.020	0.22	7.4	94	60	65	64	64
Group-5											
TC13	3.4	0.53	0.36	0.021	0.16	7.2	79	50	67	56	74
Group-6											
TC6	2.9	1.70	0.33	0.026	0.10	7.9	98	43	59	119	57
Group-8											
TC1	3.7	0.91	0.34	0.030	0.11	6.9	62	52	61	101	69
TC3	3.4	0.60	0.37	0.024	0.11	7.1	60	42	79	65	75
TC8	3.2	0.40	0.30	0.022	0.11	6.5	71	41	71	37	55
TC9	3.2	0.59	0.31	0.024	0.14	7.2	53	47	61	64	102
TC10	3.2	0.68	0.37	0.023	0.10	6.8	64	82	70	70	118
TC16	3.4	0.51	0.44	0.023	0.14	7.4	87	41	66	60	65
Group-15											
TC1a	3.0	1.40	0.40	0.017	0.06	6.5	94	106	-	70	-
TC2a	3.3	1.53	0.35	-	0.21	7.7	112	151	57	59	76

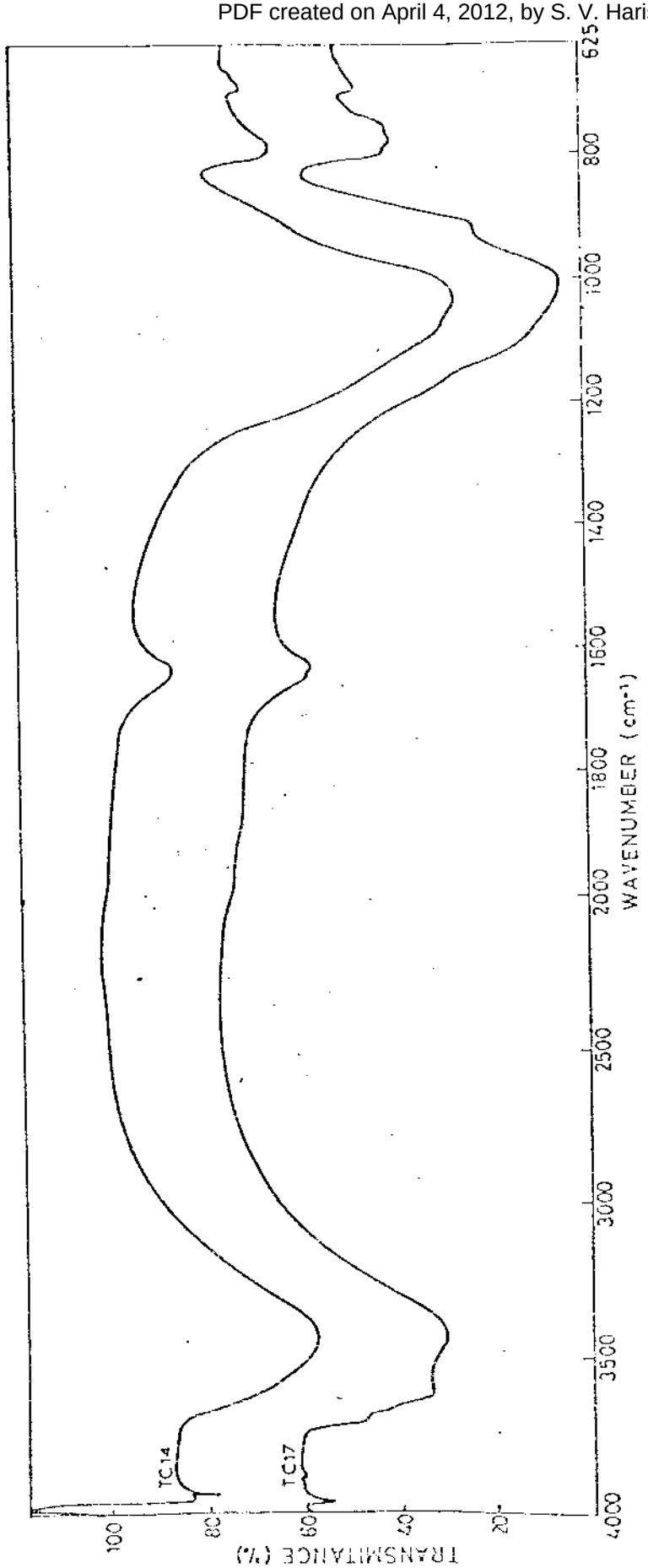

Fig. 1.

Trace elements analysis of human hair and blood serum

A. Hadjiantoniou[+], A. Katsanos, and A. Venetsianos[++]

The objectives of this work is by utilizing the well established method of the PIXE analysis (external beam technique)[1,2] to analyze various biological samples such as human hair, nail, blood serum for trace elements.

The biological samples are collected from selected individuals in order to have a representative cross section of the greek population. Samples are preferably collected from persons living in polluted environments. This will enable us to establish the average (normal) content and distribution of trace elements in the above mentioned biological samples and furthermore to establish any existing correlation between health disorders and variations in the concentration of the trace elements.

This work consitutes a part of the IAEA coordinated research programm under the title "Nuclear methods in health related monitoring of trace element pollutants.

In the framework of this investigation a collaboration has been established with the Mental Health Hospital of Athens for the study of trace elements in hair and blood serum samples of mentally disturbed persons (schizofrenics). Hair and blood serum samples are collected from patients and the staff of the hospital who live in the same environment.

[+]Health Physics Div., NRC Democritos
[++]Dromokaition Sanatorium, Athens.

References

1. A. Katsanos, A. Xenoulis, A. Hadjiantoniou and R.W. Fink, Nucl. Instr. and Meth. 139 (1976) 119
2. A. Katsanos and A. Hadjiantoniou, Nucl. Instr. and Meth. 149(1978) 469.

A study of the biological damage of protons at different energies

A. Peris[+], E. Sideris[++], A. Katsanos , and Gr. Pontifex[+]

The aim of this work is to study the results when various biological systems are irradiated with protons of various energies and therefore of various LET, (Linser Energy Transfer). Proton beams with energies from 2 to 10 MeV from the Tandem van de Graaff are used for these experiments. The beam hits a gold target, and the elastically scattered protons at small angles are passing through a thin window into the air to irradiate the petri-dishes containing the samples.

The petri-dishes that contain monolayers of cells from Chinese Hamster are placed opposite to the window of the scattering chamber and perpendicular to the proton trajectories.

Dosimetry is done by calculating the dose on the cells on the basis of the protons known LET as well as their current density which is measured during the experiment. After the irradiation of the cells, the DNA of which has been labeled with radioactive thymidine, they are lysed and suspended in a sacrose gradient. Following centrifugation at 3800 rpm for one hour after which the contents of the tubes are collected as fractions. The radioactivity of each fraction is then measured and it is plotted against fraction number. The arithmetic mean of the resulting distribution depends on the dose received and on the quality of the radiation. In the figure the weighted means of such distributions have been plotted against dose and for 2.5 MeV protons as well as for γ-rays from a cobalt- 60 source. Since the weighted means reflect the degree of breaking of the DNA strands by the radiation, it can be seen from the slopes of the respective lines in the figure that protons appear to be more destructive in their capacity of breaking DNA than γ-rays.

[+]Rad. Physics Dpt. Areteion Hospital, Athens University
[++]Biology Division, NRC Democritos

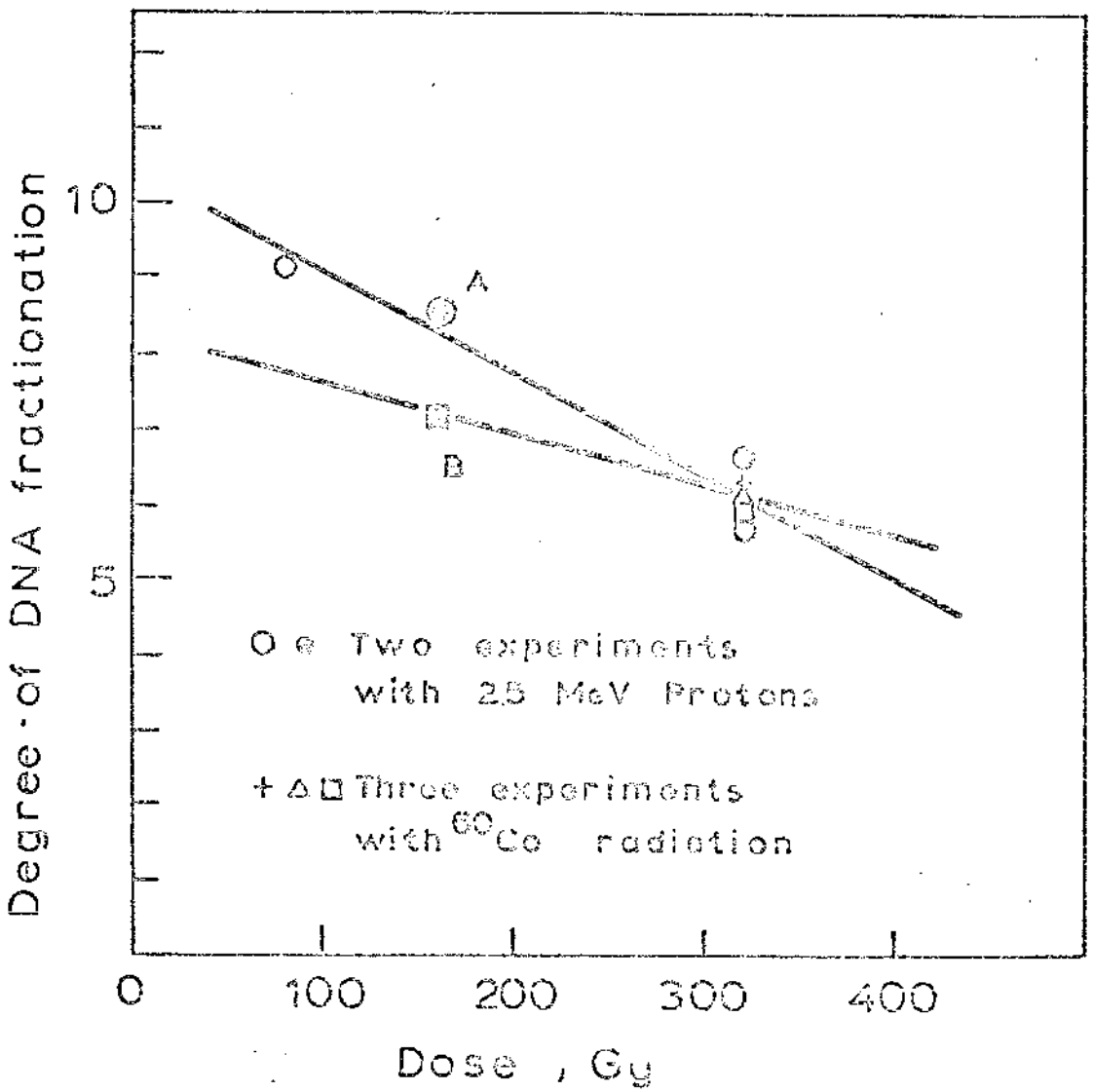

Caption to the Figure:

The results of two experiments with protons and three experiments with γ-rays. The two proton experiments have been normalized in point A and the three γ-ray experiments in point B. The straight lines have been fitted to the experimental points by eye. On the absissa are the weighted means of the fraction number of the experiments.

Bulk analysis with heavy ion beams, calibration

G. Blondiaux[+], J.O. Debrun[+], G. Costa[++], A. Katsanos, G. Vourvopoulos

Heavy ions are of interest for the profiling of light elements, but also for the determination of the bulk concentration of a number of impurities. In this last case, one either takes advantage of the coulomb barrier to determine light elements at trace level in heavy matrixes (1) or uses coulomb excitation to determine various medium weight and heavy elements in favourable matrixes, by prompt γ-ray spectrometry(2).

The accuracy of the results depends on the method of calibration, on the knowledge of the cross-sections and of the stopping powers. For bulk analysis, the method of calibration known as the "average stopping power method"(ASP) is inherently accurate (3); also, it is insensitive to inaccuracies (even large) concerning the cross-section, which need only be known in a relative manner.

Possible sources of error in the ASP are the stopping power data, which , again, need only be known in a relative manner.

It is shown in this paper that instead of using heavy ion stopping power data (experimental or semiempirical) it is possible to use hydrogen(4) or helium(5) data, with an accuracy of 1-2%.

This was verified experimentally for ^{12}C and ^{16}O ions and for Ti and TiFe, TiCu TiNi alloys, at ∿ 1 MeV/amu. This result is evidence that in the present case the approximation $S = f(v', Z_1) \cdot g(v, Z_2)$ (6) is valid with good accuracy, at least relatively. (S = stopping power - V, Z_1 speed and atomic number of the incident ion - which permits the use of H or He data of good accuracy instead of having to resort to heavy ions stopping powers which might be less accurate.

The cross-section curves or the thick target yields (relative values) are needed for the calculation of the average energy in the ASP metnod ; it is shown in this paper in two cases (Ti and Ag), that when using coulomb excitation, calculated cross-section curves are perfectly adequate. Consequently when performing ion beam bulk analysis with heavy ions and using coulomb excitation, one does not need to know the stopping power of these ions (one uses H or He data) and does not need to determine the cross - section curve (calculated curve is good enough).

References

1) J.R. McGinley, G.J. Stock, E.A. Schweikert, J.B. Cross, R. Zeister L. Zikovsky, J. of radioanal. Chem., 43(1978) 559.
2) B. Borderie, J.M. Barrandon B. Delaunay, M. Basutcu, NIM, 163 (1979) 441.
3) K. Ishii, M. Valladon, J.L. Debrun NIM, 150 (1978) 213.
4) H. H. Andersen, J.F. Ziegler, H stopping powers and ranges in all elements, Pergamon, 1977.
5) J.F. Ziegler, He stopping powers and ranges in all elements, Pergamon, 1977.
6) J.F. Ziegler, Appl. Phys. Lett., 31, n° 8 (1977) 544.

+CNRS, Service du Cyclotron-3A rue de la Ferollerie - 45045 Orleans CEDEX (France)
++ CNRS, Centre de recherches nucleaires, Strasbourg (France)

Stopping power effects in the determination of ^{14}N by a resonance reaction

A.C. Xenoulis, C.E. Douka[+], T. Paradellis and A. Katsanos

The applicability of the $^{14}N(p,p'\gamma)\ ^{14}N$ nuclear reaction in the determination of the absolute abundance of ^{14}N, with 2% uncertainty, was demonstrated at 4.3 MeV bombarding energy. The fact that almost all of the thick-target γ-ray yield resulted from a resonance at Ep= 4.0 MeV, allowed us to consider the necessary stopping-power corrections only at the energy of that resonance. Alternatively, the method was used to obtain the stopping power of 4.0 MeV protons in complex biological materials.

[+]Department of Soils and Plant Nutrition, NRC Demokritos

Microanalysis of Si via the ^{28}Si (p,p'γ) reaction

A.C. Xenoulis and A. Aravantinos

In a thin-target excitation function study of the reaction $^{28}Si(p,p'\gamma)$ between 2.7 and 3.7 MeV, an isolated resonance was identified at 3.1 MeV bombarding energy. A similar excitation function was obtained with a thick target also, since it is expected that a realistic sample will be a thick one.

These data indicate that an appropriate bombarding energy for Si microanalysisis at 3.3 MeV, with which one is ensured that almost all of the γ-ray yield will result from the 3.1 MeV isolated resonance.

A complication with the proposed reaction arises from the observation that in case the sample will contain Al, the reaction $^{27}A(p,\gamma)$ ^{28}Si will interfer with the previous reaction. In order to be able to account for this interference, an excitation function of the γ-ray yield associated with the reaction ^{27}Al (p,γ) was measured using a thick Al target. This excitation function was found to vary smoothly and increase very slowly with bombarding energy, These data demonstrated that the Al interference can be accounted for by measuring the ^{27}Al (p,γ) reaction below the 3.1 MeV resonance and subtracting its contribution extrapolated at the actual bombarding energy used in the Si analysis.

Effect of biological nitrogen fixation on the elemental composition of plants

C.E. Douka[+] , A.C. Xenoulis and T. Paradellis

It is known that the symbiotic action of rhizobia on a plant permits the latter to obtain and utilize atmospheric nitrogen. Our intention was to determine whether this symbiotic nitrogen fixation affects the concentration of other elements of the plant as well. For that purpose the elemental composition of leaves of Medicago Sativa grown with or without active rhizobia meliloti under similar otherwise conditions of growth was determined and compared. The elemental composition was determined via the XRF technique. This comparison indicated that the concentration of certain elements in the leaves is indeed affected by biological nitrogen fixation. Specifically, the concentration of K and Rb was found to increase while that of Ca, Mh, Br, Sr and Mo to decrease with the interaction of the plant with effective rhizobia meliloti.

[+]Department of Soils and Plant Nutrition, NRC Demokritos

Bromine absorption from air by plant leaves

T. Paradellis and N. Panayotakis[+]

Trace elements present in the leaves of "Populus"grown in the city of Athens (group I) have been determined by XRF and compared with the corresponding concentration of elements in leaves of trees grown in the suburbs of Athens where the traffic conditon is lower (group II) and with similar trees grown far from the city (group III). The results of the work show a manyfold increase in the bromine content of the leaves in trees grown in the city. The increased presence of this element is attributed entirely to the increase of the bromine content in the air of the city due to the car exhaust, from which the leaves take this element.

In table I the measured average concentration of the trace element are given for the three groups of samples, while in fig.1 the ratio of concentrations in groups I and II to with respect to group III are shown.

Table I

Average concentration of trace elements in leaves of Populus (in $\mu g/g$ dry weight)*

Element	Group I	Group II	Group III
K	21 000 ± 3000	16 000 ± 4000	19 000 ± 3000
Ca	17 000 ± 3000	20 000 ± 2500	12 000 ± 2000
Mn	130 ± 20	130 ± 30	120 ± 40
Fe	150 ± 20	100 ± 30	110 ± 20
Cu	12 ± 4	11 ± 3	16 ± 2
Zn	100 ± 40	130 ± 40	90 ± 20
Pb	36 ± 10	20 ± 10	16 ± 6
Br	640 ± 150	200 ± 50	15 ± 6
Sr	63 ± 10	55 ± 7	35 ± 8

*±1 standard deviation of the mean.

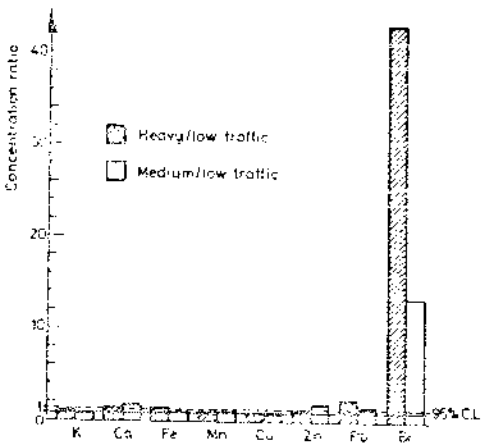

Fig. 1

[+]Syngrou Hospital, Athens.

Routine analysis of biological materials by XRF

T. Paradellis and G. Gregoriades+

Methods have been developed during the past two years for the rapid and accurate trace element analysis of biological materials.

For human sera routinely 5mℓ of serum are dopped with 1mℓ of an Y salt of 28 μg/mℓ concentration. The solution is dried and consequently burnt at about 450-500°C. The resulting ash (about 40 mg) is pressed to a pellet. To determine the self absorption effects of the samples, experimental curves are used which relate the absorption coefficient of the sample with the weight of the resulting ash in mg/mℓ . This simple connection of the absorption coefficient with the weight of the sample is a consequence of the rather constant composition of the human serum in major elements (C,O,Cℓ, Na).

For other biological fluids (bile, gastric juice, etc) this relation does not hold since these fluids can have different degrees of dilution and so a separate measurement of the absorption coefficients of the sample for each case is required.

The same arguments hold for human tissues, burnt with the same procedure. Here the major factor for fluctuations of the absorption coefficient arises from the different amount of connective tissue present in the sample. We have found that for the XRF method, the most suitable form of handling the data is the burning of the material as described above. The only major disadvantage of the mentod is theloss due to votalization of the elements As and Se. For all other measured elements we have found that any losses occurring are less than 3%

A nice example of the importance of the method in medical applications is shown in Fig. I.

The first spectrum in Fig.1 shows the trace elements observed in a sample of normal liver tissue obtained from a patient suffering from primary cancer of the rectum with an extensive metastatic cancer in the liver.

From the biopsies performed it was known that the secondary liver cancer was of the metastatic type originating from the rectum. The microscopic picture showed intestinal cells with extensive presence of calcite crystals in the samples of the liver cancer.

In Fig. I on the right side a tabulation of the measured quantities of the various trace elements are given. This values (except for Fe) are consistent with known values of trace elements of normal liver. The The presence of MO, and Mn in considerable quantities must also be noted. These two trace elements are essential for the function of the liver.

The second and third spectra in Fig. I are from the metastatic liver cancer and from the rectum cancer tissues. Immediately one sees that the elements Mo and Mn caracteristic of the liver cell are absent from the two lower cells. In addition the concentration of the elements in the two lower spectra in Fig. I are to similar that they are hardly distinguishable. If is also interesting that the large quantity of Calcium observed in the liver metastatic cancer is in agreement with the results of the biopsy.

+1st Surgical Clinic, Athens University, Medical School

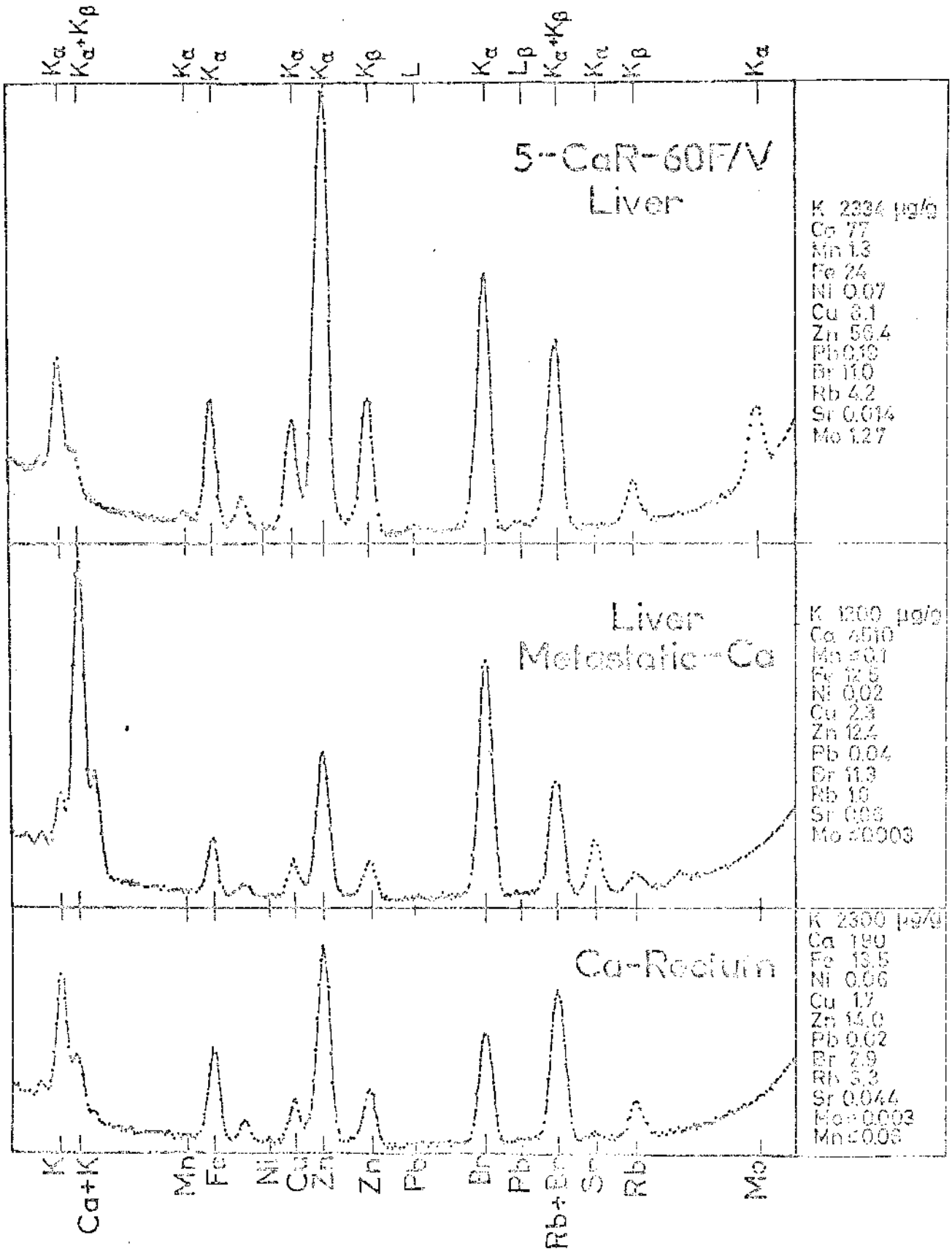

Fig. 1

*Changes of serum bromine in patients undergoing surgery**

G. Gregoriades [+] and T. Paradellis

In this study XRF methods have been applied to determine serum Br pre and post operationaly in patients undergoing surgery under total anaesthesia . As reference witnesses, patients undergoing simple herniorraphy under local anaesthesia have been used.

It has been found that patients undergoing anaesthesia with drugs very rich in Br (Fluothane) show post operative Br levels 10 times larger than the preoperative levels.

It has been also noticed that these patients show intense signs of Bromismus (Bromine poisoning) manifasting with change of physical and mental behavior. Until now this kind of post operative behavior was attributed to the postoperational stress.

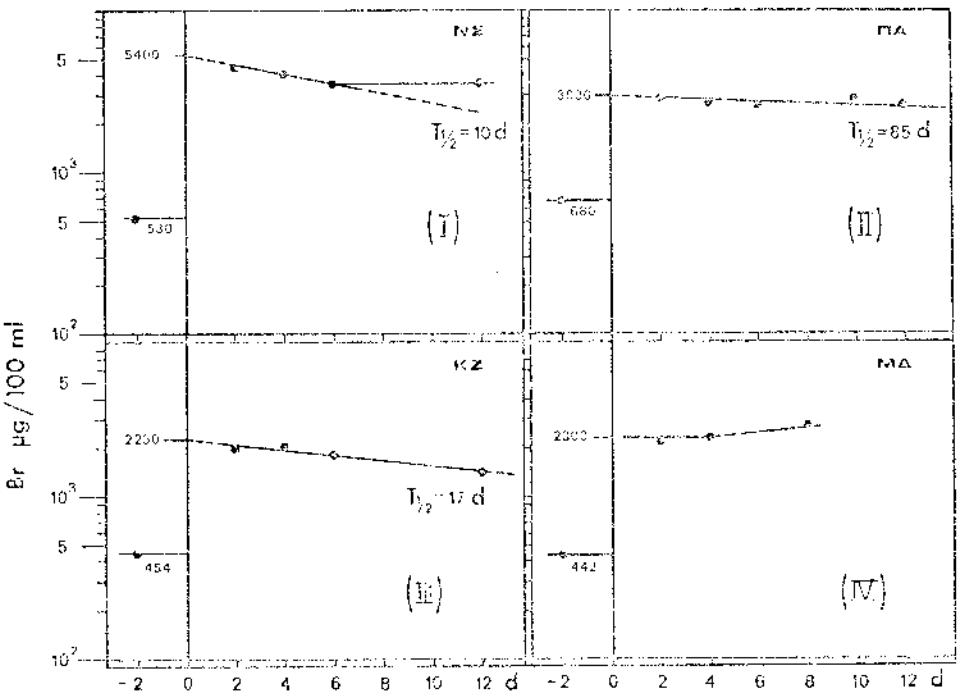

Some examples of the variation of Br levels in sera of patients who underwent surgery with total anaesthesia with drugs very rich in Br.

*Part of a wider clinical research conducted with Prof. A. Romanos, and Dr. Apostolides of the Athens University Medical School.

[+]1st Surgical Clinic, Athens University Medical School.

*Changes in composition of dental alloys after repeated castings**

N. Kafoussias + and T. Paradellis

Au-Pt alloys used for dental purposes have been analyzed by XRF to determine elemental composition. The same samples have also been analyzed after repeated castings. From the data obtained it was concluded that the greatest loss of elements during the repeated castings occured for Copper and Zinc. The changes in concentration of the elements has been correlated with the changes in other measured mechanical properties of the alloy (Tensile strength, elongation, yield strength and hardness).

* Part of a Ph.D.thesis, Dental School, University of Athens

+ University of Athens, Dental School.

Trace elements in fluids and drugs used in total parenteral nutrition[*]

N. Legakis[+] , T. Paradellis

Trace elements have been determined in various fluids and drugs used in total parenteral Nutrition (Aminoacids, Vitamins, Insulin, electrolyte solutions etc).

The major finding of this work was that the concentration in Cu and Zn (both essential elements for man) is too low in these fluids and not sufficient to meet the average daily requirements of man.

In clinical practice no effect has been observed in patients from this low presence of Cu and Zn and the reason was attributed to the fact that in all cases a relatively small time of parental nutrition has been applied (2 weeks) followed by blood transfusion. In addition the inevitable use of insulin to regulate the glucose metabolism of patients proved to be a major source of Zn input due to the relatively large quantities existing in insulin emulsions. For example it has (been found that insulin regular has about 19 μg/m& Zn while Insulin Zinc suspension about 110 μg/m& .

* Part of a Ph.D. thesis, Athens University Medical School

+ 1st Surgical Clinic - Athens University Medical School.

A survey of catalysts for the oxidation of SO_2 in dusts settled on marble monuments

D. Skiotis[+], T. Paradellis, V. Katselis

XRF has been used to determine trace elements in the atmosphere, dust and soil samples obtained at two greek archeological sites namely the Acropolis of Athens and the archeological site of Elefsis. Three of the metals which can catalyze the oxidation of SO_2 to SO_3 resulting in the sulfation of the marble surface (Fe,Mn,Pb) have been quantitatively determined in this work.

In one of the dust samples obtained form the surface of marble pieces in Elefsis the Fe content was found to be 3%. Up to treatment of 1gm of the dust with 100mℓ of distilled water a solution was obtained with a molarity with respect to the iron of 5.7×10^{-6}M. This number is six time higher than the concentration found to catalyse the oxidation of sulfur dioxide in the atmosphere.

In view of the present observations it is advisable to minimize in pratice the quantity of dust deposited on marble monuments in order to reduce their deterioration due to sulfation.

[+] On leave of absence from the Royal Melbourne Institute of Technology.

*Magic numbers as a result of symmetry limitations of many-nucleon angular momenta**

G.S. Anagnostatos

Whereas the empirical evidence for spin-orbit coupling is certainly strong, it is not certain that it is brought about by a term $f(r)\ \vec{\ell}\ \vec{s}$ for the individual nucleons[1], and moreover, it is not certain that its magnitude is of the right order to explain the observed level split at N or Z = 50,82, and 126[2]. We have found in an unambiguous way that the symmetry limitations of the orbital angular momenta of many nucleons are the cause of this significant energy split, while the spin-orbit coupling simply coexists: This effect would persist even if the spin-orbit coupling was not present. Specifically, while up to $\ell=3$ for each ℓ the symmetries of a specific high symmetry equilibrium[3] polyhedron are sufficient to describe all $2\ell+1$ independent axes of orbital angular momentum $\vec{\ell}$, for $\ell = 4,5$, and 6 two such polyhedra are needed. One is needed for the $\ell + 1$ axes and another of lower symmetry for the ℓ axes. These axes may facilitate $2(2\ell + 1)$ and $2(\ell)$ nucleons all with spin parallel and spin antiparallel, respectively. This effect constitutes the origin of the observed large level split at the high magic numbers.

These findings become even more important in the framework of the isomorphic model[4], where the magic numbers correspond to nucleon numbers equal to cumulative numbers of vertices (standing for nucleon average positions) of successive concentric equilibrium[3] polyhedra shells with the correct quantum states.

References

* Work supported in part by the Public Benefit Foundation Alexander S. Onassis

1) M.G. Mayer and J.H.D. Jensen; Elementary Theory of Nuclear Shell Structure (Chapman and Hall, Ltd., London, 1955), pp. 59-60.

2) D. Inglis and S. Dankoff, Phys. Rev. 50, 783, 784 (1936); G. Breit, Phys. Rev., 51, 248, 778 (1937), 52, 546 (1937); A.M. Feingold, Ph.D. Thesis, Princeton University, 1952; E.P. Wigner, address at conference in Rio de Janeiro, 1952.

3) J. Leech: Math. Gaz., 41, 81 (1957).

4) G.S. Anagnostatos : Can. J. Phys., 51, 998(1973) Atomkernenergie, 29, 207 (1977); Lett. Nuovo Cimento, 22, 507 (1978); 28, 573 (1980); 29, 188 (1980) and G.S. Anagnostatos, S. Touliatos, A. Kyritsis and J. Yapitzakis : Atomkernenergie, 35, 60 (1980)

Nucleon distributions and a two-nucleon potential for high-energy heavy-ion collisions[*]

G.S. Anagnostatos and C.N. Panos[+]

Nucleon distributions and a two-nucleon effective potential are presented and are suitable for high-energy heavy-ion collisions, e.g. through the classical equation of motion approach[1,2]. Our distributions are made of concentrically arranged equilibrium[3] polyhedra shells in close packing and are consistent with many nuclear properties, e.g. magic numbers [4], nuclear density[4], nuclear radii[4-6], electric quadrupole moments[5,6], angular momenta[7], Coulomb[5] and binding[8] energies. Using these initial distributions, we have derived the two-nucleon potential which reproduces very well, for the first time, both the nuclear binding energies (for the correct nuclear sizes) and the first two moments of the differential nucleon-nucleon scattering cross-section at high energies (i.e., the longitudinal momentum loss cross-section and the transverse momentum transfer cross-section). Specifically, our potential has the form of a two-term Yukawa potential, i.e.

$$V_{ij} = V_R \frac{e^{-\mu_R r_{ij}}}{r_{ij}} - V_A \frac{e^{-\mu_A r_{ij}}}{r_{ij}} ,$$

where V_R, V_A, μ_R, and μ_A are the four parameters of the potential and r_{ij} is the relative distance between any two nucleons i and j. These parameters can be expressed in terms of the following four independent and more physical parameters: r_c, the soft core radius of the nuclear potential ; r_m, the radius where the minimum of the potential occurs ; V_m, the depth of the potential ; and $\nu = \mu_R - \mu_A$. The best values found for these independent parameters are: $r_c = 1.13$ fm, $r_m = 1.21885$ fm, $V_m = -27.5$ MeV, and $\nu = 30.5$ (see Fig. 1).

This potential is applied; first to our nucleon distributions for all closed - shell nuclei with $N \geq Z$ and the following binding energies (in MeV) are found.

^{4}He: 27.1 (23.3), ^{16}O: 118.1 (127.6), ^{40}Ca: 368.0 (342.1). Their good agreements with the experimental values (given inside parentheses) are apparent. Second to NN high energy scattering and the following values for the first two moments, $\sigma^{(1)}(E)$ and $\sigma^{(2)}(E)$, of the differential scattering cross-section are found: $\sigma^{(1)}/\sigma^{(2)}(E)$: 10.86/10.61, 6.28/6.21 4.65/3.93 4.17/3.26 and 3.92/2.84, respectively to the projectile laboratory energies E_L = 50, 100, 200, 300, and 500 MeV, which values for both moments and for the whole range of energies E_L, for the first time, are almost within the experimental errors of n-p and p-p empirical data[9,10](see Fig. 2)

---

* Work supported in part by the Public Benefit Foundation Alexander S. Onassis

+ Physics Department, University of Ioannina, Ioannina, Greece

References

1 A.R. Bodmer and C.N. Panos, Phys. Rev. C15, 1342 (1977)

2 A.R. Bodmer, C.N. Panos, and A.D. Mackellar, Phys. Rev. C22, 1025(1980)

3 J.Leech, Math. Gaz. 41, 81 (1957).

4 G.S. Anagnostatos, Can. J. Phys. 51, 998 (1973).

5 G.S. Anagnostatos, Atomkernenergie 29, 207 (1977)

6 G.S. Anagnostatos, S. Touliatos, A. Kyritsis, and J. Yapitzakis, Atomkernenergie 35, 60 (1980).

7 G.S. Anagnostatos, Lett. Nuovo Cim. 22, 507 (1978); 28, 573 (1980); 29, 188(1980).

8 G.S. Anagnostatos, Proceedings of the International Conference on Nuclear Physics, edited by J.De Boer and H.J. Mang Vol 1 (Munich, 1973) p.101.

[9] R.A. Arndt, R.H. Hackman, and L.D. Roper, Phys. Rev. C9, 555 (1974) and references therein.

[10] A. Rindi, C.B. Lim and T. Salmon-Cinotti, Lawrence Radiation Laboratory Report No. UCRL-20295, Nov. 1970 (unpublished) and references therein.

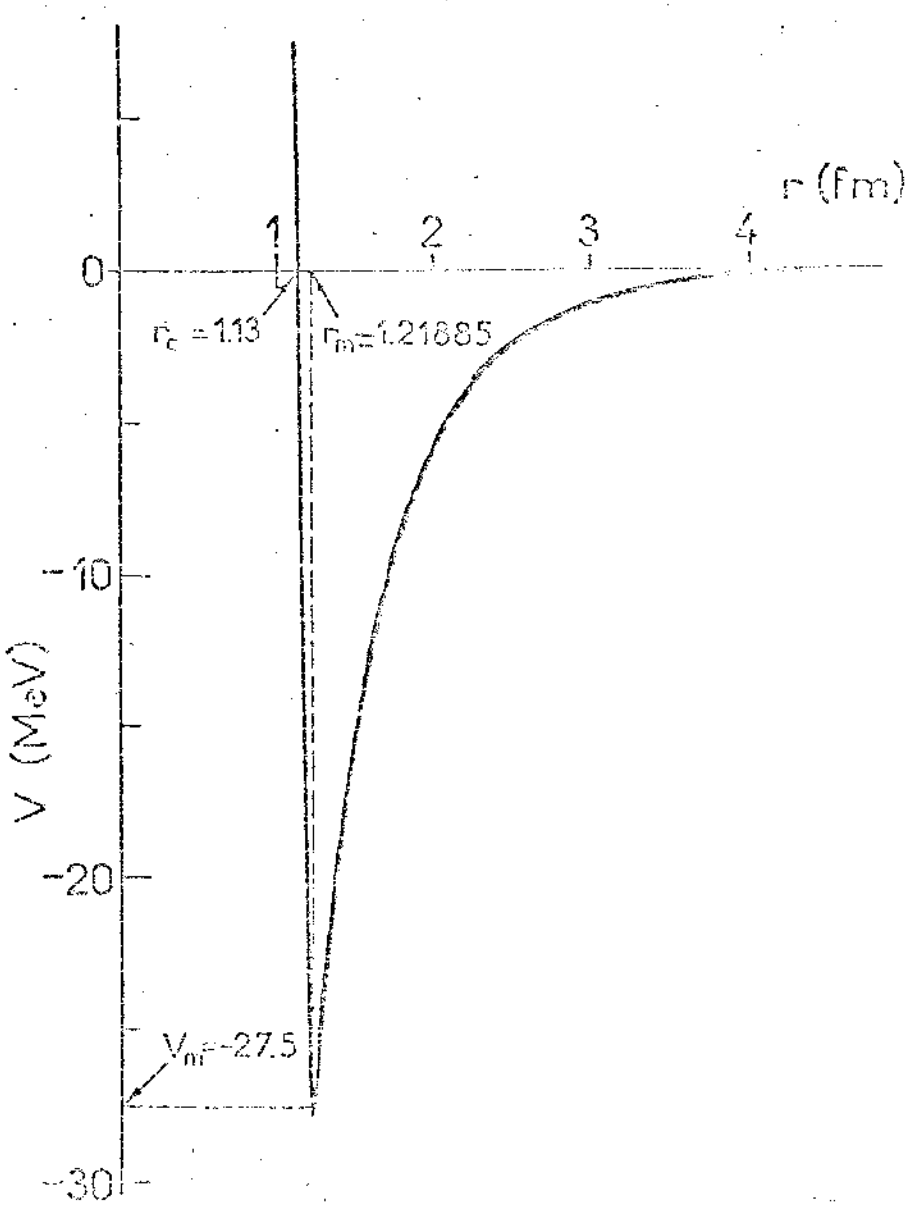

Fig. 1

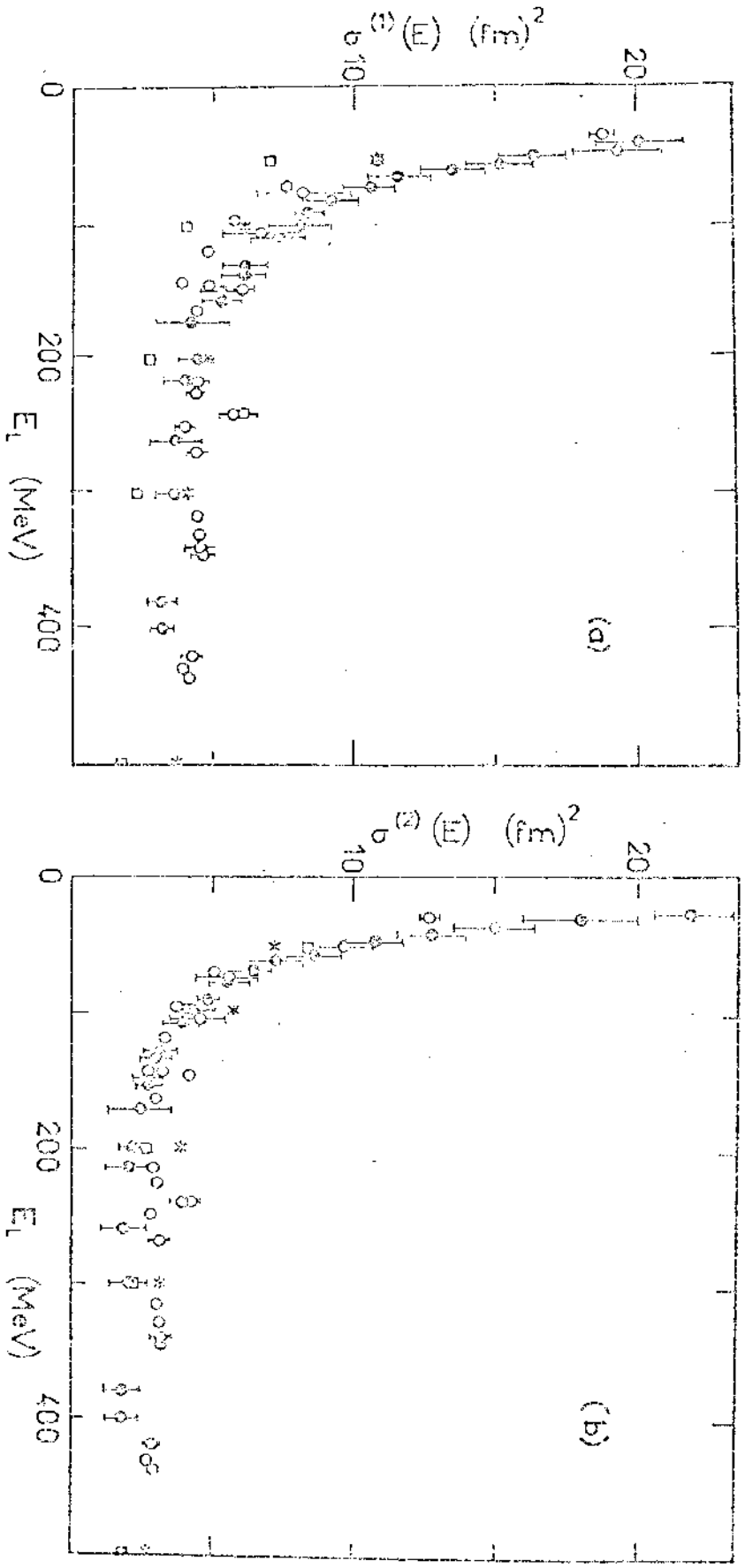

Fig. 2

*Rotational invariance of orbital angular momentum quantization of direction for degenerate states**

G.S. Anagnostatos, J. Yapitzakis[+], and A. Kyritsis[++]

The conservation of angular momentum is a consequence of central forces in both classical and quantum physics. In addition in quantum mechanics, we have the quantization of direction of angular momentum coming as a result of quantization of both the angular momentum itself and its projection on the z-axis. This quantization of direction for the one-body problem leaves the angles φ unspecified, while it specifies the azimuthal angle θ according to the formula

$$\theta_{\ell}^{m} = \cos^{-1}\left(m/\sqrt{\ell(\ell+1)}\right) \qquad (1)$$

In the case of the many-body problem, however, it seems that both angles θ and φ are specified, as a result of the restrictions imposed on each particle from its neighbor particles.

In a previous publication ([1]) we have noticed that (concerning ℓ values from 1-4 and partially 5) the specification of both θ and φ in the orbital-angular momentum quantization of direction (OAMQD of many non-interacting particles in a central potential) is related to the regular and quasi-regular polyhedra. In the present paper we have exhausted the subject of finding such pairs of θ and φ angles for all ℓ values from 1 to 6, and moreover we have determined the symmetry properties of the relevant orbital angular momentum vectors $\vec{\ell}$.

In fig.1 the quantization of direction for ℓ= 1-6 and all associated m values (m= $-\ell,\ldots,+\ell$) is shown in relation to cubic - octahedral symmetry. Specifically, the relevant vectors (shown in scale for each block in fig.1) defined by the angles θ_{ℓ}^{m} (see eq. (1)) are shown in two sets of m values (for reasons to be understood shortly; row 1 and 2) and for all m values together (row 3) with respect to an octahedron, a cube (hexahedron) or a cube-octahedron, i.e. with respect to polyhedra of the cubic-octahedral group. The choice of the specific polyhedron shown in each case was made with reference to the clarity.

Possible other vectors in fig.1 with equal θ_{ℓ}^{m} are obvious.

For all parts in fig.1 ((a) - (r)), the z-axis has the same direction. Actually, it is aligned to the direction from the center to the middle of an edge of the octahedron (fig.1(a)) with respect to which all other polyhedra are oriented. The $\bar{\ell}$ vectors, forming the appropriate θ_{ℓ}^{m} angles in any order of accuracy ([1]), pass through characteristic points of the polyhedra employed in fig.1 which are marked with a solid circle throughout the figure. Specifically, these points for $\ell=1$ are the vertices of an octahedron for both sets of m values (fig.1(a)-(b)); for $\ell = 2$ the vertices and the shown golden section point of a cube (fig.1(d) and (e), respectively) ; for $\ell = 3$ the middles of edges of a cuboctahedron for both sets of m (fig.1(g)-(h)) ; for $\ell = 4$ the vertices of an octahedron (fig.1(j) and the vertices of a cuboctahedron (fig.1(k)); for $\ell=5$ the middle points of the shown line segments of an octahedron (fig. 1(m)) and of a cuboctahedron (fig.1(n)), and for $\ell = 6$ the third of the shown line segments of a cube (fig.1(p)) and the middle points of the shown line segments of a cuboctahedron (fig.1(q)).

The main feature of the $\bar{\ell}$ vectors of any of the two sets of m values (that is, the vectors of either row 1 or row 2) for each ℓ is that they transform into each other, and only to them, through symmetry operations of the cubic-octahedral group. But while this is true for each of the two sets separately, except for $\ell = 1$ and 3, the one set is not transformed into the other set by any symmetry operation of this group (They use different characteristic points). The difference between the case $\ell = 2$ and the cases $\ell = 4$-6 is that all $\bar{\ell}$ vectors of only the former (fig. 1(f)) transform into each other through some of the operations of the (I) group. (That is, not all operations of the (I) group lead to permissible directions of $\bar{\ell}$). Thus finally, for $\ell = 4$-6 only there are not symmetry operations transforming the one set of $\bar{\ell}$ vectors into the other. That is, for these ℓ values we do not have one but two degenerate QAMQD.

It is of great interest to notice that the number of $\bar{\ell}$ vectors in row 1 and row 2 for each ℓ value is equal to $\ell + 1$ and ℓ, respectively. That is, considering particles processing spin, we see that these two sets of $\bar{\ell}$ vectors are equal to those needed for particles with spin and orbital angular momentum parallel $\{2(\ell+1)\}$ and anti-parallel (2ℓ) respectively. This fact is particularly important for the cases ℓ=4-6 (which have a split of degeneracy in QAMQD with $\ell+1$ and ℓ QAMQD degenerate members), since

it implies (even without spin consideration) a similar split in energy degeneracy of the $2\ell+1$ states, if a different radial wave function for each set of $\vec{\ell}$ vectors (rows 1 and 2) is assumed, e.g., according to the isomorphic model ([2]), where the relevant $\ell+1$ and ℓ vectors correspond to two different size polyhedral shells. In such a case, the known spin-orbit coupling effect is merely added into the previous independent effect of energy split, reported here for the first time.

In rows 3 and 4 of fig.1 (i.e. in fig. (1) (ℓ)', (o), (r) and (v)-(x)), as shown, we present the relative orientation of the polyhedra employed in order to help the reader visualize the relationship between the symmetries of the two sets of $\vec{\ell}$ vectors in rows 1 and 2. In addition in row 4 of the figure, some auxiliary material is presented to make the relationships among polyhedra of the (O) group obvious and also to show the alternative choice of z-axis and characteristic points in equivalent representations of $\vec{\ell}$ vectors.

In conclusion, we have found that the degenerate states of the same ℓ value have a rotational invariance of QAMQD which splits into two sets with $\ell+1$ and ℓ members for ℓ=4-6. The latter fact of QAMQD split recommends a further study for a re-examination of the strong spin-orbit coupling explanation of magic numbers in Nuclear Physics.

In general, we may say that the presented QAMQD implies the existence of a fundamental symmetry in nature which (with previous findings([1,3]) could be used as a basis of a physical theory of the structure of matter.

---

*Work supported in part by the Public Benefit Foundation Alexander S.Onassis.

(1) G.S. Anagnostatos : Lett. Nuovo Cimento 22, 507 (1978) .

(2) G.S. Anagnostatos : Can. J Phys. 51 , 998 (1973); Atomkernenergie 29, 207 (1977) ; and G.S. Anagnostatos, S.Touliatos, A. Kyritsis, and J. Yapitzakis : Atomkernenergie 35 , 60 (1980)

(3) G.S. Anagnostatos: Lett. Nuovo Cimento 28, 573 (1980); and 29, 188(1980).

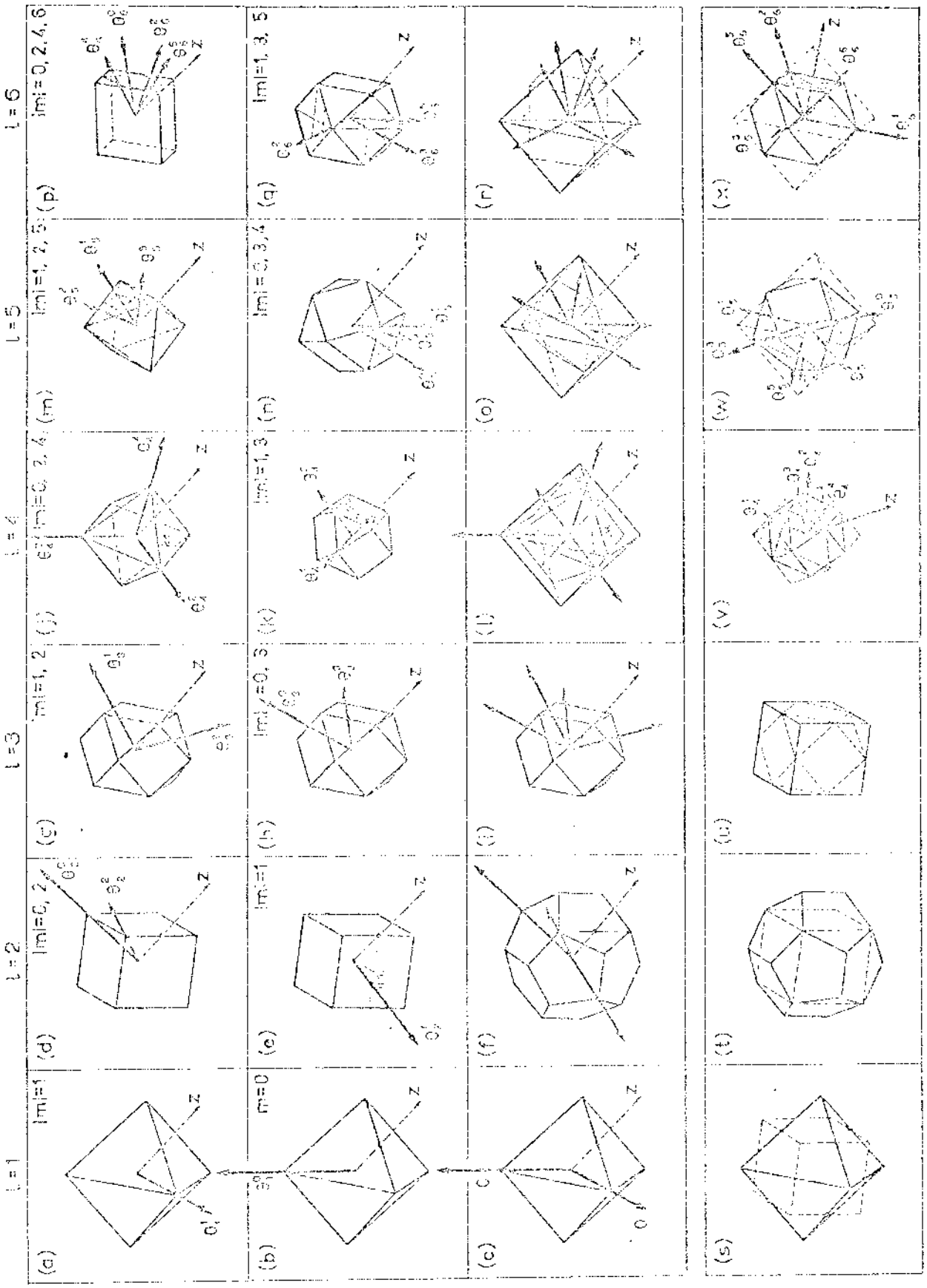
l = 1
l = 2
l = 3
l = 4
l = 5
l = 6
(a)
(b)
(c)
(d)
(e)
(f)
(g)
(h)
(i)
(j)
(k)
(l)
(m)
(n)
(o)
(p)
(q)
(r)
(s)
(t)
(u)
(v)
(w)
(x)
|m|=1
m=0
|m|=0, 2
|m|=1, 2
|m|=0, 3
|m|=1, 3
|m|=0, 2, 4
|m|=1, 2, 5
|m|=0, 3, 4
|m|=1, 3, 5
|m|=0, 2, 4, 6
z

Fig. 1

Initial values of parameters for variable-moment of inertia models

G.S. Anagnostatos, K. Demakos, and A. Vassiliou[+]

The study of rotational or quasirotational spectra in even-even nuclei is of great importance in Nuclear Physics. In the framework of a phenomenological treatment of these spectra, the study is limited to a functional fitting of the energies of the spectrum so that the energy equation

$$E_I = V_I + T_I \qquad (1)$$

and the equilibrium condition

$$\frac{\partial E_I}{\partial \vartheta} = 0 = \frac{\partial V_I}{\partial \vartheta_I} + \frac{\partial T_I}{\partial \vartheta_I} \qquad (2)$$

are satisfied for each state of the spectrum with angular momentum I. It has been found [1] that the moment of inertia (ϑ) is the most appropriate independent variable (Variable-Moment-of-Inertia (VMI) models) in the expressions for the potential energy part (V_I) and for the kinetic energy part (T_I) of the rotational excitation energy (E_I)

Usually, the kinetic energy has the same form for all versions of the VMI model, i.e.

$$T_I = \frac{I(I+1)}{2\vartheta_I}, \text{ (where } \hbar^2 \text{ is taken equal to 1),} \qquad (3)$$

whereas the potential energy varies from version to version, i.e., it includes one or more terms from the expansion of the potential round the ground state value (ϑ_0) of the independent variable ϑ_I. Thus, in the most general case it has the form

$$V_I = C_0 + C_1(\vartheta_I - \vartheta_0) + C_2(\vartheta_I - \vartheta_0)^2 + \ldots \qquad (4)$$

Thus, from the computing point of view, the subject is the determination

of the parameters C_i and ϑ_o using eqs. (1) and (2) in such a way that the model predictions reproduce the experimental energies with the least squared error. As known, such a fit (involving a nonlinear system of equations) is very sensitive to the initial values of these parameters. The purpose of the present paper is to provide such initial values.

We start with the approximate expression (2) for the moment of inertia

$$\vartheta_I(\text{initial}) \cong \frac{2I - 2}{E_I - E_{I-2}}, \tag{5}$$

(where E_I stand for the experimental energy of the spectrum with angular momentum I) and we estimate, using eqs. (1) and (3), approximate values for the potential energy (V_I) for each value of the angular momentum (I), i.e.,

$$V_I \cong E_I\ (\text{exp}) - \frac{I\ (I+1)}{2\vartheta_I} \tag{6}$$

Thus, for each I value of the spectrum, we have a pair of approximate V_I and ϑ_I in the V_I, ϑ_I plane. Then, for all I we apply first a least-square technique to determine a complete polynomial of the form

$$V_I = \alpha_o + \alpha_1\vartheta_I + \alpha_2\vartheta_I^2 + \ldots\ldots \tag{7}$$

(to fit all V_I, ϑ_I pairs) and then a polynomial of the form

$$V_I = A_o + A_1(\vartheta_I - \vartheta_o) + A_2(\vartheta_I - \vartheta_o)^2 + \ldots\ldots, \tag{8}$$

where ϑ_o is the value of ϑ_I for I = 0 from eq. (9)

$$V_I = \alpha_o + \alpha_1\vartheta_I + \alpha_2\vartheta_I^2 + \ldots\ldots = 0, \tag{9}$$

and $\vartheta_I - \vartheta_o$ implies a translation (of ϑ_o units) of ϑ_I axis.

The value of A_o is expected to be equal to zero, but it usually takes a small non-zero value as a result of statistics in the least-square procedure. The higher order term in eq.(7) or (8) depends on the version of the VMI model we consider. After that, using eqs.(3) and (8), we solve eqs.(1) and (2) to determine trial values of E_I (model) and ϑ_I(model). Now, the ϑ_I(model) values (instead of those from eq. (3)) are inserted in eq. (6) and new polynomials V_I from eqs. (7) and (8) are determined,

which with eqs. (1), (2), and (3) lead to new trial values E_I(model) and ϑ_I(model). This procedure continues until we have no meaningful changes in E_I(model) from one cycle to the next.

Given that A_0 and A_1 always have a very small influence in the fitting, as initial values of C_2, C_3, and C_4, for the least squares fit in the different versions of the VMI model, we take the values of the corresponding coefficients of the last polynomial V_I of eq. (8), e.g., for the VMI234 version,

$$C_2(\text{initial}) = A_2,\ C_3(\text{initial}) = A_3,\ \text{and}\ C_4(\text{initial}) = A_4.$$

The procedure previously described for determining initial values of parameters has been successfully applied to almost all known nuclear rotational spectra and no problem of convergence has been observed.

+ Computer Div., NRC Democritos

[1] M.A. J. Mariscotti, G. Scharff-Goldhaber, and B. Buck, Phys. Rev. 178 (1969) 1864.

[2] A. Johnson, H.Ryde, and S.A. Hjorth, Nucl. Phys. A179 (1972) 753.

V. DATA COLLECTION AND PROCESSING - DEVELOPMENT

Elemental analysis of XRF-spectra

V. Katselis

A program has been written for the analysis of XRF-Spectra. The spectra are collected with a TN-1700 analyser which allows processing of the stored data with a BASIC program. Special BASIC functions access analyser parameters such as calibration factors and cursor positions.

For each peak the peak position and left and right limits are given with a cursor (BIG) from the display. The energy is obtained from the peak position and is used to identify the element with the aid of a stored table of energies of characteristic X-rays. The table covers the elements from chlorine to Bismuth.

The background is obtained with linear interpolation between the limits. It is then subtracted from the total counts to yield net counts.

Finally the information on the durationof the measurement is accessedand the intensity (in counts per second) is computed.

All this information is printed on the Teletype in tabular form. An option is included for the analysis of small peaks sitting on the tail of larger ones. The program has sifnificantly reduced the time needed for sample analysis with the XRF-method.

Installation of the K-3000 accelerator

A. Katsanos, G. Prokos and A. Asthenopoulos

The success of the Proton Induced X-ray Emission program with applications in various fields led us to a decision to create an independent unit for this project. For this purpose we acquired from another division of our center an old K-3000 van de Graaff electron accelerator. The main accelerator has already been assembled in our laboratory and we are now in the process of changing it to a proton machine, to be used for the above mentioned program.

Quadrupole triplet for charged particle detection

G. Vourvopoulos, M. Greenfield[†], F. Trouposkiadis, N. Andreopoulos, O. Topikoglou

For the detection of charged particles from the (n,p) and (n,α) reactions, a quadrupole triplet system has been chosen, to focus the charged particles 3m away from the target. The quadrupoles have 20 cm internal diameter providing thus a solid angle of ∿ 10 msr.

The optical calculations have been performed and the carriage for rotating the quadrupole system in order to take angular distribution was designed and construction is well underway.

The quadrupoles were donated to Demokritos from C.E.N. Saclay.

[†] Florida A and M University, Tallahassee, Florida, USA

VI. ACCELERATOR OPERATION

A. Asthenopoulos, N. Andreopoulos, N. Divis, N. Iliadis, N. Papakostopoulos and G. Prokos

During 1980 the Tandem Accelerator was utilized for a total of 2185 hours. Heavy ions were employed 82% of the time and light ions 18%.

There were a total of 6 tank openings for minor repairs and foil changes. The belt has accumulated over 9000 hours of operation.

Fig. 1 shows the beam time percentage versus terminal voltage for the year 1980. Although the accelerator was used 61% of the time at potentials larger than 4 MV (3/4 of the maximum voltage), there is a 10% utilization of the Tandem at potentials less than 1.5 MV.

The diode source used for the production of light ions was replaced with a General Ionex off-axis duoplasmatron ion source. Several power supplies had to be built and a Freon 113 circulating system was constructed.

An Alcatel turbomolecular pump installed in one of the beam legs was replaced with a regular diffusion pump due to its unsatisfactory performance to attain high vacuum.

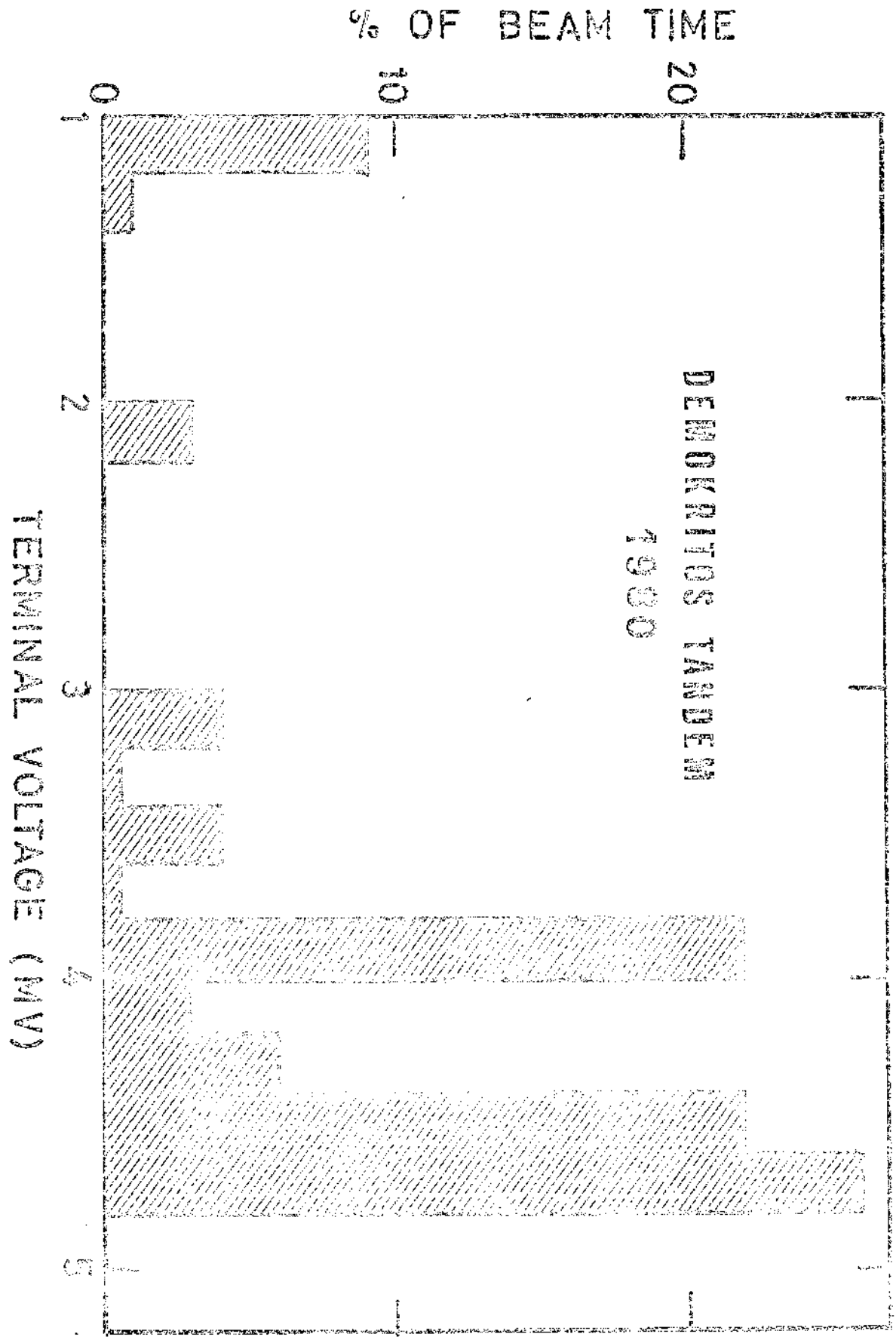

VII. PERSONNEL

Research Staff

Dr. G. Vourvopoulos, Director
Dr. G. Anagnostatos
Dr. C. Kalfas
Dr. A. Katsanos
Dr. V. Katselis
Dr. E. Kossionides
Dr. Th.Paradellis
Dr. L. Skouras
Dr. A. Xenoulis

Graduate Students

E. Adamides
A. Aravantinos
X. Aslanoglou
P. Bakoyeorgos
E. Gazis
P. Kakanis
S. Papaioannou

Scientific Associates

Prof.	G. Andritsopoulos	(Univ. of Ioannina)
Prof.	P. Assimakopoulos	(Univ. of Ioannina)
Mr.	G. Gregoriades	(Univ. of Athens)
Dr.	A. Hadjiantoniou	(N.R.C."Democritos")
Dr.	E. Mavrommati-Fountou	(Univ. of Athens)
Dr.	K. Papadopoulos	(Nat. Technical Univ of Athens)
Mr.	N. Parayotakis	(Syngrou Hospital, Athens)
Dr.	C. Panos	(Univ. of Ioannina)
Dr.	R. Vlastou	(Nat. Technical Univ. of Athens)
Mr.	J. Yapitzakis	(Univ. of Athens)

Operational Staff

Accelerator Support Group

N. Andreopoulos
A. Asthenopoulos
N. Divis
N. Iliadis
N. Papakostopoulos
G. Prokos

Electronics Group

A. Chionakis
A. Sokos

Computer Programmer

Mrs. K. Dimakou, B.S. Mathematics

Machine Shop

O. Topikoglou

Graphics

F. Trouposkiadis

Secretariat

Mrs. A. Demetriou

Visiting Scientists

Prof. M. Greenfield	*25-6 ÷ 25-10/ 80*	A and M Univ. Florida,
Dr. G. Doukellis	*1-9 ÷ 30-10/ 80*	Max Planck Institut , Heidelberg
Dr. Z. Zhelev Dr. I. Penev	*6,7,8 -5/ 80*	Inst. for Nuclear Physics, Sofia
Prof. N. Cindro Dr. E. Holub	*1÷15 /2 /80*	Rūdjer Boskovic Inst. Belgrade
Dr. G. Costa Dr. J. Lebrun	*1÷15/3/80*	Centre de Recherches Nucleaires de Strasbourg, France
Dr. R. Caplar Dr. D. Pocanic	*16-6 ÷ 10-7/80*	Rujker Boskovic Inst. Belgrade

VIII. P U B L I C A T I O N S

A. Papers published in 1980

1. G.S. Anagnostatos
   "Comments on "Extension of the variable-moment-of-inertia model to high spins"
   Phys. Rev. C22 (1980) 305

2. G.S. Anagnostatos
   "The Geometry of the quantization of angular momenta $(\bar{\ell},\bar{s},\bar{j})$ in fields of central symmetry"
   Lett. Nuovo Cimento 28 (1980) 573

3. G.S. Anagnostatos
   "A symmetry description of the independent particle model"
   Lett. Nuovo Cimento 29 (1980) 188

4. G.S. Anagnostatos, S. Touliatos, A. Kyritsis, and J. Yapitzakis
   "Quadrupole moments and rms charge radii of nuclei with $8 \lesssim Z \lesssim 60$"
   Atomkernenergie 35 (1980) 60

5. G. Andritsopoulos, X. Aslanoglou, P. Bakoyeorgos and G. Vourvopoulos
   "^{12}C - ^{12}C resonances studied through γ-decay"
   Phys. Rev. C21 (1980) 1648

6. C.A. Kalfas, E.G. Sideris, S. El-Kateb, P.W. Martin and U. Kuhnlein
   "Determination of rotational correlation times from perturbed angular correlations of γ-rays. ^{111}Indium bound to single-stranded DNA and DNA $\{Cu^{2+}\}$
   Chem. Phys. Lett. 73 (1980) 311

7. P.W. Martin, C.A. Kalfas and K. Skov
   "Study of conformational changes in Bovine Serium Albumin by perturbed angular correlations"
   Nucl. Instr. Meth. 171 (1980) 603

8. T. Paradellis, N. Panayotakis
   "Bromine absorption from the air by plant leaves
   J. Radioan. Chem. 59 (1980) 221

9. A.C. Xenoulis, E.N. Gazis, P. Kakanis, D. Bucurescu and A.D. Panagiotou, "Competition between exit channels leading to the same residual nucleus in heavy - ion reactions"

Phys. Lett. 90B (1980) 224

10. Y. Maniatis and A. Katsanos
"Relative Dating of Bones from Thessaly"

Anthropos 7 (1980) 136

B. Papers accepted for publication to appear in 1981

1. E. Adamides, L.D. Skouras and A.C. Xenoulis
   "Structure of low-lying states in ^{94}Mo"
   Phys. Rev. C

2. E.N. Gazis, P. Kakanis and A.C. Xenoulis
   "The contribution of unbound deuteron disintegration to the reaction ^{12}C(^{16}O,pn) ^{26}Al
   Phys. Rev. C

3. D. Pocanic, G. Vourvopoulos, X. Aslanoglou and E. Holub
   "Possible evidence for the existence of intermediate resonant structure in the ^{9}Be + ^{13}C heavy-ion system"
   J. Phys. G

4. D. Skiotis, T. Paradellis and V. Katselis
   "A survey of catalysts for the oxidation of SO_2 in dusts settled on marble monuments
   Clean Air

5. A.C. Xenoulis, C.E. Douka, J. Paradellis and A. Katsanos
   "Stopping power effects in the determination of ^{14}N by a resonance reaction"
   J. Rad. Chem.

C. *Conferences - Reports -Dissertations*

1. G.S. Anagnostatos
"The Geometry of the independent particle model"
Inst. Phys. Conf. on "Trends in Nuclear Structure Physics",
Manchester, England, April 1980.

2. G.S. Anagnostatos
"The symmetry of angular momentum imposes limitations on the independent particle model"
Int. Conf. on Nucl. Phys., Berkeley, U.S.A. August 1980.

3. G.S. Anagnostatos and C.N. Panos
"The angular structure of nuclei from Deuteron to Carbon"
European Symposium on Few Body Problems in Nuclear and Particle Physics, Sesimbra, Portugal, June 1980.

4. G.S. Anagnostatos and C.N. Panos
"A two-nucleon potential"
2nd Panhellenic Conf. of the Greek Physical Society, Mytilini Greece, Sept. 1980.

5. X. Aslanoglou, G. Vourvopoulos, D. Pocanic and E. Holub
"Low energy resonances in the system $^{9}Be + ^{12}C$"
Conf. on the Resonant Behavior of Heavy Ion Systems, Aegean Sea, Greece, June 1980.

6. R. Caplar, G. Vourvopoulos, X. Aslanoglou, D. Pocanic, G. Andritsopoulos and P.W. Martin.
"Search for intermediate resonances in ^{36}Ar via the $^{12}C + ^{24}Mg$ entrance channel.
Winter meeting on Nuclear Physics, Bormio, Italy, Jan. 1980.

7. C.E. Douka, A.C. Xenoulis and T. Paradellis
"Study of interaction between microorganisms and environment by the XRF technique"
Int. Symposium on Microbiol. Ecology, Coventry, England, Sept. 1980.

8. C.A. Kalfas
"Current research in Nuclear Physics in Greece (Review paper).
2nd Panhellenic Conf. of the Greek Physical Society, Mytilini,
Greece, Sept. 1980.

9. B. Kargas, E. Mavrommatis
"Jastrow - type calculations for "nuclear matter"with correlation
functions obtained by means of a differential equation"
Inst. Conf. on Nucl. Phys., Berkeley, U.S.A., August 1980.

10. N. Legakis, Gr. Gregoriades, N. Apostolides, A. Romanos and T.
Paradellis
"Trace elements in fluids and drugs administered intravenously"
XII Conf. of the Greek Surgical Society, Athens, Greece, Oct. 1980.

11. D. Pocanic, G. Vourvopoulos, X. Aslanoglou and E. Holub.
"Resonance indications in the $^{9}Be + ^{13}C$ system"
Conf. on the Resonant Behavior of Heavy Ion Systems, Aegean Sea
Greece, June 1980.

12. A. Romanos, Gr. Gregoriades, N. Apostolides and T. Paradellis.
"Changes of Serum Bromine in patients undergoing surgery"
XII Conf. of the Greek Surgical Society, Athens, Greece, Oct. 1980.

13. D. Skiotis, T. Paradellis, V. Katselis
"Catalytic oxidation of SO_2 on marble surface"
3rd Intern. Congress for the deterioration and preservation of building
stones, Venetia, Oct. 1979.

14. G. Vourvopoulos, X. Aslanoglou, C.A. Kalfas, N. Cindro, E. Holub,
D.M. Drake, J.D. Moses, J.C. Peng, N. Stein and J.W. Sunier
"^{30}Si studied via the $^{18}O(^{12}C,\alpha)$ and $^{16}O(^{14}C,\alpha)$ reactions"
Conf. on the Resonant Behavior of Heavy Ion Systems, Aegean Sea,
Greece, June 1980.

15. G. Vourvopoulos, X. Aslanoglou, C.A. Kalfas, E. Holub, N. Cindro, D.M. Drake, J.D. Moses, J.C. Peug, N. Stein and J.W. Sunier
"Resonances in ^{30}Si system studied via the $^{18}O(^{12}C,\alpha)$ and $^{16}O(^{14}C,\alpha)$ reactions"
XIIIMasurian Summer School, Mikolajki, Poland, Sept. 1980.

16. P. Egelhof, B. Bauer, R. Boettger, S. Kossionides, K.H. Moebius, Z. Moroz, D. Presinger, R. Schuch, E. Steffens, G. Tungate, W. Dreves, I. Koenig, D. Fick.
"Polarized Heavy Ion Beams ($^{6,7}Li$, ^{23}Na) at the Heidelberg EN-Tandem"
Fifth Int. Symposium on Polarization Phenomena in Nuclear Physics, Santa Fé, New Mexico, U.S.A., 1980.

17. I. Koening, D. Fick, R. Boettger, P. Egelhof, H. Ingwersen, S. Kossionides, K.H. Moebius, D. Pressinger , E. Steffens
"Production of vector polarized nuclei by ^{7}Li Beams"
Fifth Int. Symposium on Polarization Phenomena in Nuclear Physics, Santa Fé, New Mexico, U.S.A., 1980.

---

1. G.S. Anagnostatos and C.N. Panos
"Angular Momenta (ℓ,s,j) in fields of central symmetry and regular polyhedra"
Greek AEC, DEMO report 80/8, 1980.

---

1. E.N. Gazis
"Competition between exit channels producing the same residual nucleus in heavy ion reactions"
Ph.D. Thesis, University of Athens, 1980
Laboratory advisor: Dr. A. Xenoulis; Professor : A. Panagiotou.